JETS FROM HADRON-, MUON-, NEUTRINO INTERACTIONS IN COMPARISON WITH JETS FROM e^+e^- ANNIHILATION

D. Haidt

Deutsches Elektronen-Synchrotron
DESY
Hamburg, Germany

I. INTRODUCTION

Jets are a typical high energy phenomenon observed about 30 years ago in cosmic ray interactions. Fig. 1 shows a prominent example (P1). In contrast to the cosmic ray stars they were given the name "explosion showers" or "jets". Various early models, e.g. FERMI's isotropic fireball model (F1), HEISENBERG's shock wave model (H1), LANDAU's hydrodynamic model (L1), later HAGEDORN's thermodynamical model (H2), attempted an understanding of the simplest features such as particle production, multiplicity, inelasticity distributions. Low statistics and difficulties in the event reconstruction limited a fast progress. At 1952 still only 8 complete jets with energies ranging from 20 to 30 000 GeV were available (H3).

With the advent of high energy accelerators a systematic study of many body final states set in. The energies available at the beginning were much too small to exhibit jets. A large number of new hadrons was discovered and ordered in multiplets. The success of the 8-fold way suggested the existence of a quark triplet, the fundamental representation of the underlying SU(3) symmetry. Experimental searches for such elementary building blocks failed. Another, rather direct way to the question of whether there exist any elementary constituents within the nucleon was proposed by BJORKEN (B1): lepton scattering at high momentum transfers is a unique probe of short distances. As a matter of fact, soon afterwards the SLAC-MIT deep inelastic electron proton experiments (P2,M1), later muon and neutrino experiments, supported approximate BJORKEN scaling (B1,B2) of the nucleon structure functions. In the parton model (B3,F2) these findings were interpreted as scattering off pointlike constituents, called partons by FEYNMAN. The comparison of deep inelastic neutrino and electron scattering led to the identification of partons with fractionally charged quarks (D1). Furthermore, the evaluation of the integral over the second neutrino nucleon structure function, which measures the momentum fraction carried by quarks and antiquarks, turned out to be only 0.49 ± 0.05 (E1) suggesting the existence of yet another kind of partons, called gluons, within the nucleon.

Despite the successes of the parton model its application to the hadronic final states remained doubtful. Most attractive were speculations about the process $e^+e^- \to$ hadrons (B4). At high enough energies the parton model would, together with the observation of limited transverse momenta in hadron-hadron collisions (C1), suggest the appearance of jets. Several years later, when the SPEAR e^+e^- collider came into operation, the jet character of the final state hadrons could indeed be demonstrated (H4). At the much higher PETRA energies jets become visible even to the naked eye (fig. 2).

The Intersecting Storage Ring, ISR, opened up a new energy domain in proton-proton collisions. Contrary to expectation the measurement of the transverse momentum distribution of single hadrons

revealed an energy dependent tail (fig. 3), (D2). This was interpreted as resulting from a hard scattering process. After many years of experimentation the occurrence of opposite sided high P_T jets could be claimed (S1).

More data in deep inelastic lepton nucleon scattering proved that BJORKEN scaling was only an approximate concept. The pattern of the deviation from scaling could be understood within QCD, which attempts the description of the parton dynamics. At the same time, the dynamical fundament of the parton model induced new questions. For instance, the elementary gluon bremsstrahlung process should manifest itself in a gluon jet. The 3-jet events observed at PETRA (S2,P5) are interpreted as being due to this process.

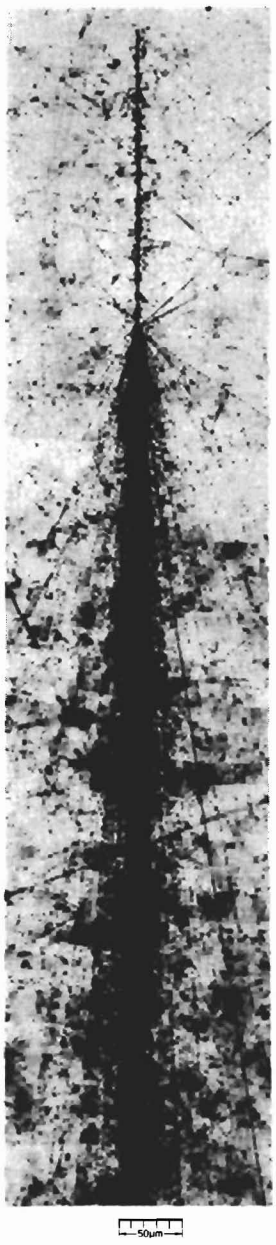

In conclusion, the development over the last three decades has revealed a strong interplay between various hard scattering processes and the occurrence of jets.

The subject of jets and their comparison is so vast that restrictions to some aspects seemed to be demanded. For further reading a few review articles are quoted at the end.

Fig. 1: Collision of a primary iron nucleus, of about 5000 GeV per nucleon, in a nuclear emulsion on balloon. There are about 200 charged particles in the final state.
(Courtesy of Prof. D. Perkins)

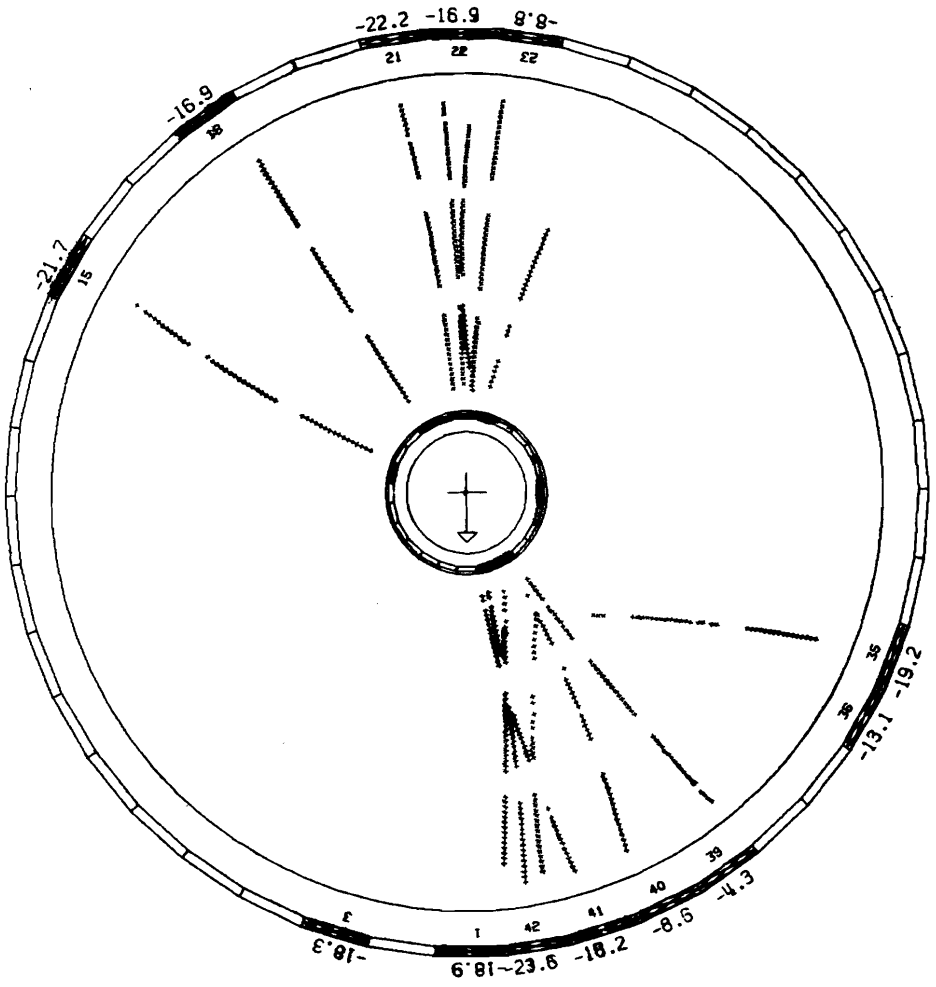

Fig. 2: High energy electron-positron annihilation event at PETRA observed in the JADE detector. The multibody final state shows a clear two-jet structure.

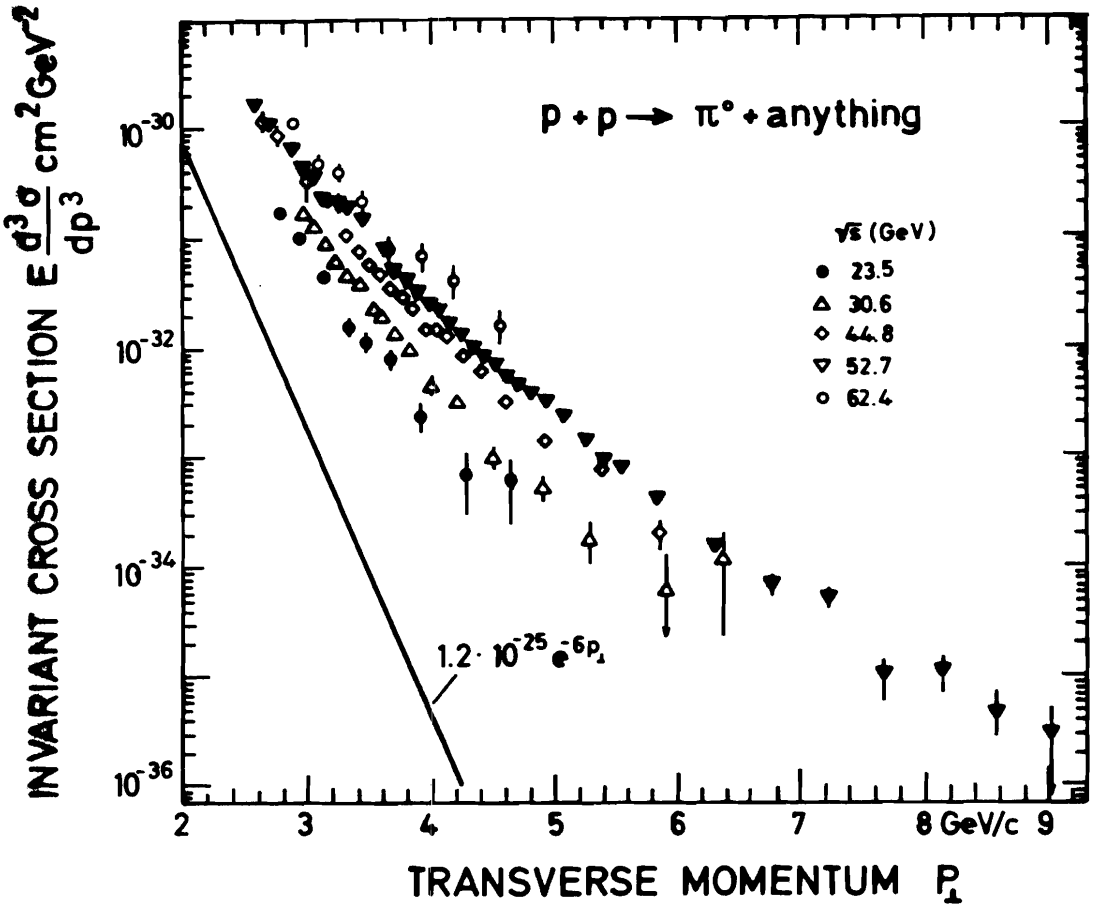

Fig. 3: Inclusively produced π^0 in pp interactions at high transverse momenta are much more abundant than expected on the basis of the low P_T behaviour. The effect increases with increasing energy.

II. THE JET PHENOMENON

As a first and rough approach the multiplicity and sphericity aspect will be considered. The sphericity of an event consisting of n hadrons is defined by:

$$S = \frac{3}{2} \min_{\vec{e}} \frac{\sum_{i=1}^{n} (\vec{P}_i \times \vec{e})^2}{\sum_{i=1}^{n} \vec{P}_i^{\,2}} = \frac{3}{2} \min_{\vec{e}} \frac{\langle P_T^2 \rangle}{\langle P^2 \rangle}$$

The minimization procedure results in an axis oriented along $\vec{e}$ or $-\vec{e}$ and a value S between 0 and 1. As a property of nature $\langle p_T^2 \rangle$ stays approximately constant. Thus, jets manifest themselves, provided $\langle p_T^2 \rangle \ll \langle \vec{p}^2 \rangle$. This condition is not satisfied at low energies. But also at high energies care has to be exercised: events with low multiplicity will have a badly determined axis (fig. 10), and events with high multiplicity approach the phase space limit (see fig. 7 in reference B8).

Fig. 4 compares three hard scattering processes within the naive parton model: electron-positron scattering via 1 photon exchange, lepton-nucleon deep inelastic scattering (νN, $\bar{\nu} N$, $\mu^{\pm} N$, $e^{\pm} N$) and hadron-hadron deep inelastic scattering. Except for the first process only part of the energy is available for jet production. Table 1 summarizes the effective energy for the various reactions. In lepton nucleon scattering the effective energy is the invariant mass of the hadron system: $W^2 \approx 2ME(1-x)y$, where E is the energy of the initial lepton, M the nucleon mass and x, y the BJORKEN scaling variables. For a given E the effective energy is governed by the shape of the nucleon structure functions and by the y-distribution.

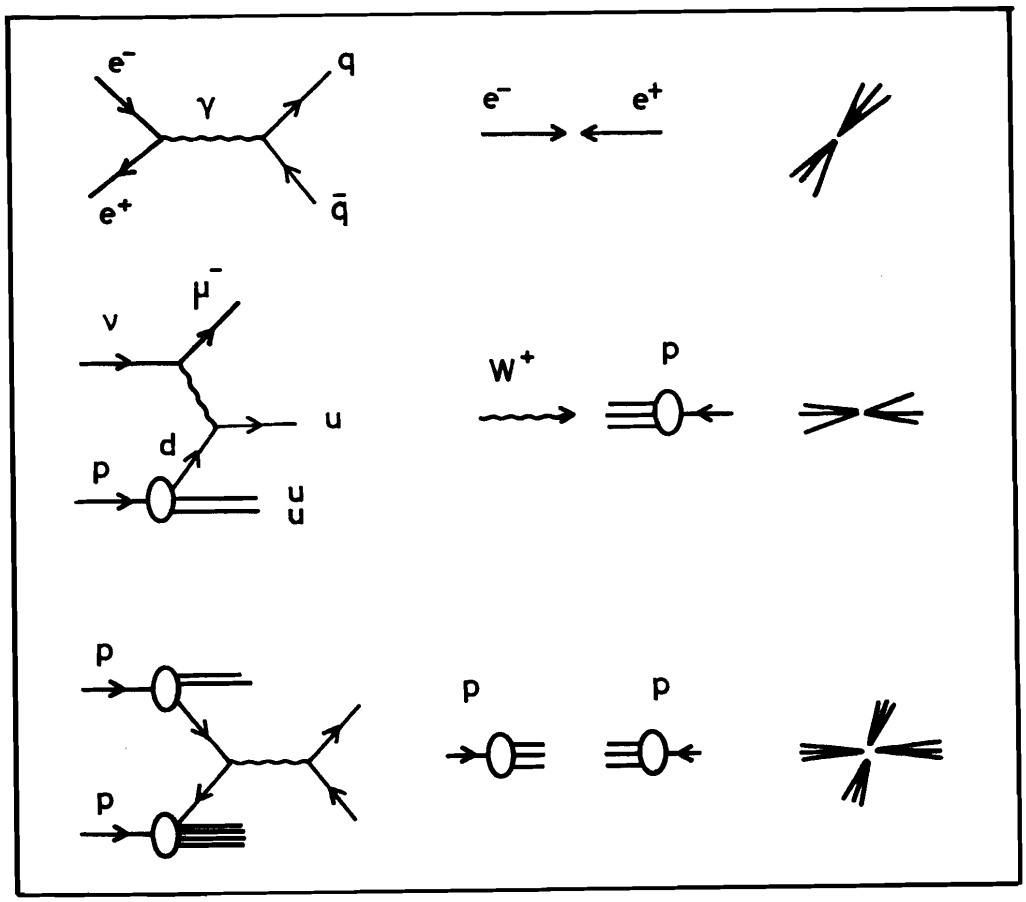

Fig. 4: Comparison of three hard processes

Beam	$\sqrt{s}$ /GeV	$\sqrt{s_{eff}}$/GeV
e^+e^- PETRA	36	36
ν NB SPS	15	9
ν WB SPS	9	5
μ EMC SPS	23	14
ISR pp	62	15
hh SPS	24	5

Table 1: Comparison of the energy effectively available for jet production at various accelerators.

Contrary to e^+e^- interactions ℓN processes have a built-in axis, since the intermediate vector boson (y, Z^0, $W^\pm$) induces the jets. Furthermore, choosing the variable x in the valence region neutrino induced jets are pure u-jets and antineutrino induced jets pure d-jets. Most complicated is the hadron-hadron interaction, where the structure functions enter twice. Denoting by x_1, x_2 the fractional momenta of the participating quarks the energy available for the subprocess giving rise to the transverse jets is: $\sqrt{s_{eff}} = \sqrt{s}\ \sqrt{x_1 x_2}$. Obviously, high values can only be obtained, if the quarks belong to the tail of the valence structure functions and this is very rare.

Multiplicity

The average charged multiplicity in e^+e^- interactions observed up to PETRA energies is displayed in fig. 5, (F3). Note that K^0_S decaying in $\pi^+\pi^-$ are included. The energy dependence of the data is well represented (F3) by

$$\langle n_c \rangle = a + b \exp(c\ \ell n \frac{s}{\Lambda^2})$$

with $a = 2.05 \pm 0.22$ $\quad b = 0.027 \pm 0.013$

$c = 1.97 \pm 0.13$ $\quad \Lambda \equiv 0.3$

Various attempts have been made to compare the mean charged hadron multiplicities in e^+e^- with ℓN and hh collisions. Using $\sqrt{s_{eff}} = W - M$ in ℓN and $\sqrt{s_{eff}} = \sqrt{s} - m_h - m_{h'}$ in hh' (A1) the data lie approximately on a universal curve for energies up to about 10 GeV. Recent data on νp (A2) and $\bar{\nu}p$ (B5,A3) are compared with e^+e^- in fig. 6. The systematic difference may be attributed to the difference in the total hadronic charge, which is 2 for νp and 0 for $\bar{\nu}p$. The mean charged multiplicity in νp scattering depends only upon W and is independent of Q^2 (fig. 7) (A2).
The parton model (fig. 3) suggests that the multiplicity in deep inelastic scattering gets different contributions from forward and backward fragmentation. This is borne out in comparing $\bar{\nu}p$ with $\bar{\nu}n$ data (B5) in fig. 8.

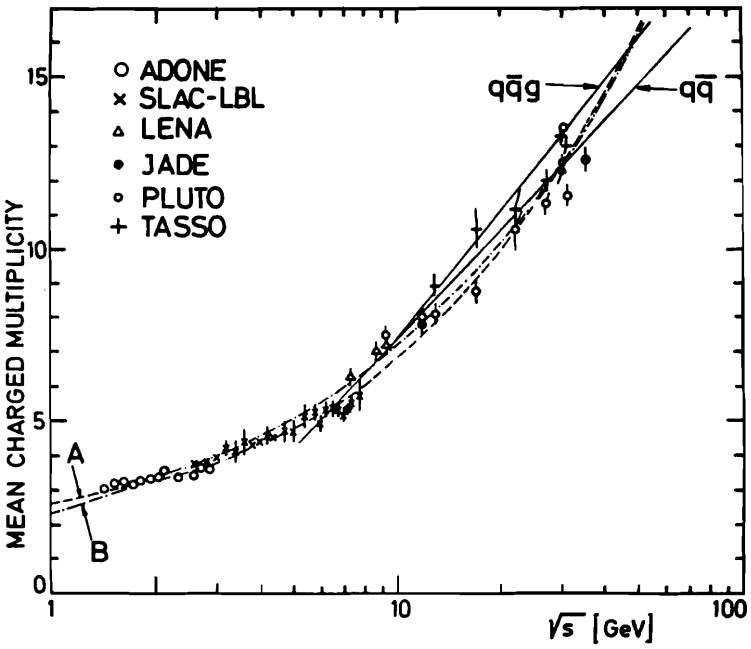

Fig. 5: Average multiplicity in e^+e^- annihilation as a function of the centre of mass energy.

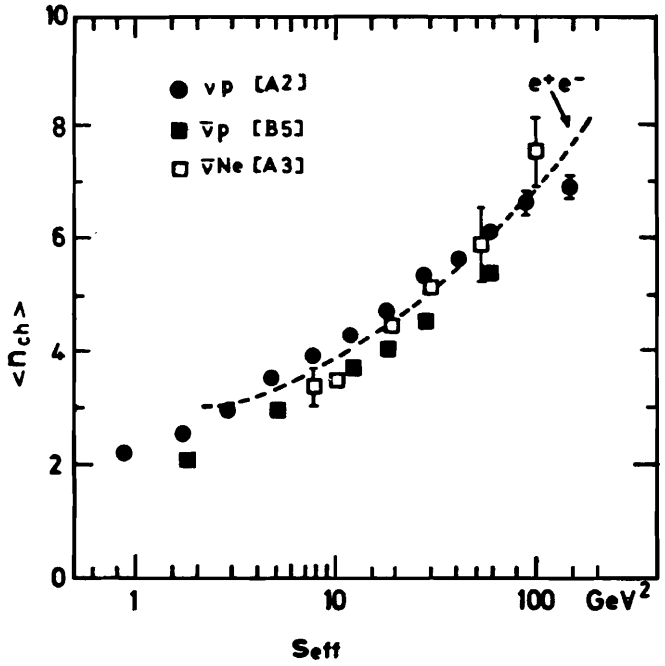

Fig. 6: Comparison of the mean multiplicity observed in neutrino and antineutrino experiments with e^+e^-. The dotted curve is taken over from fig. 5.

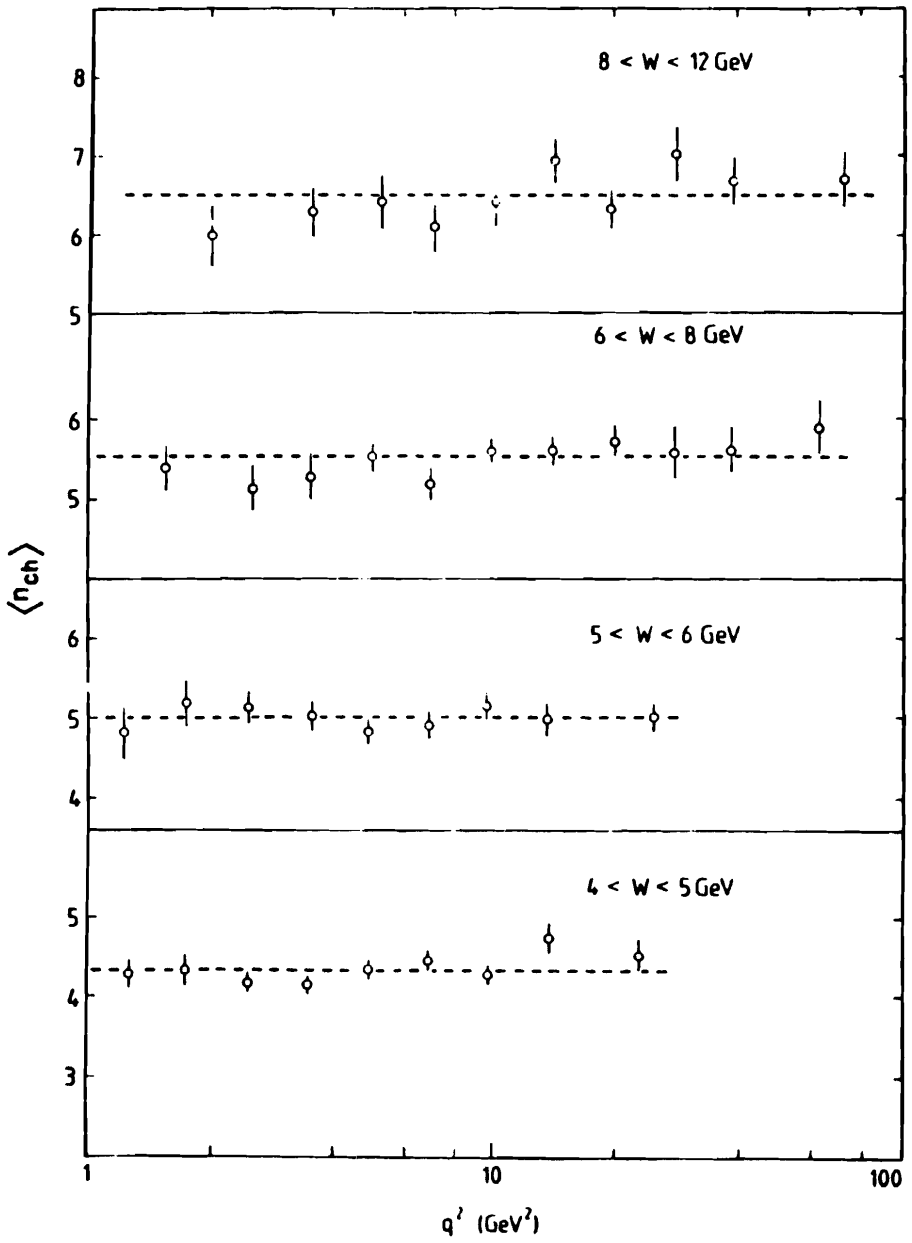

Fig. 7: The mean multiplicity in νp scattering depends only upon the invariant mass of the total hadron system. The data of the BEBC collaboration (A2) are shown.

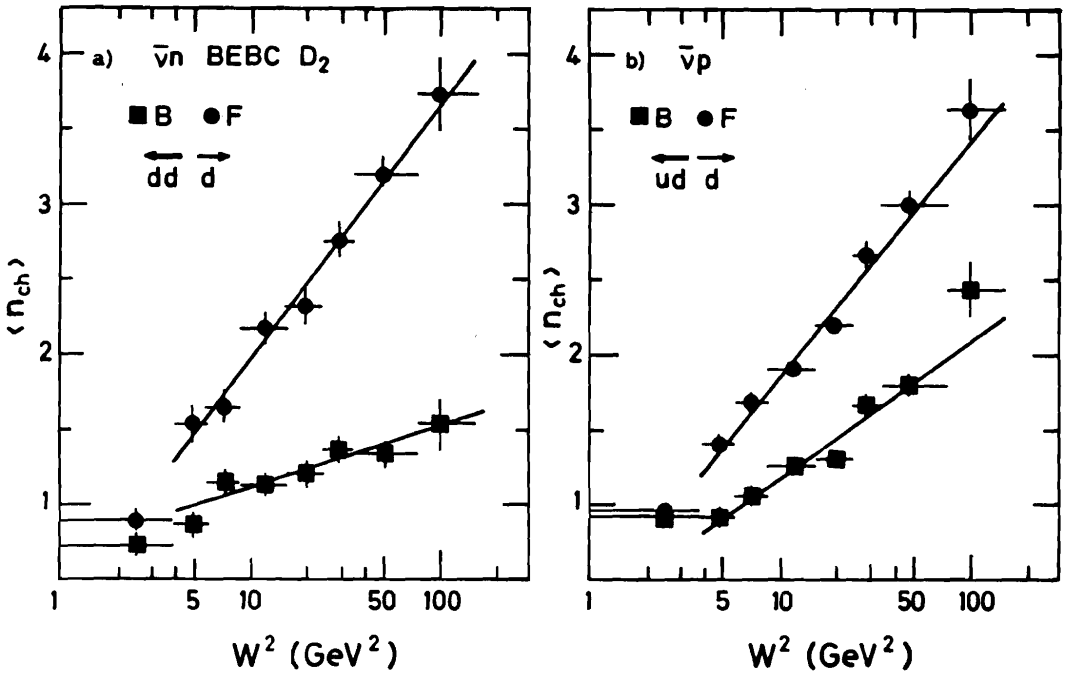

Fig. 8: Average charged multiplicity in νn and $\bar{\nu}$p interactions separately for forward (F) and backward (B) jets in the total hadron centre of mass system.

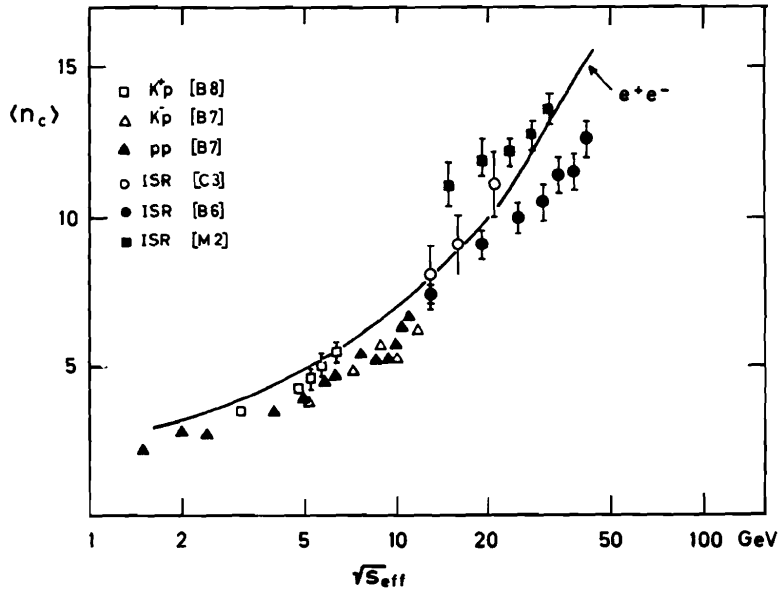

Fig. 9: Comparison of mean multiplicities in low and high P_T hadron-hadron experiments with e^+e^-. The curve is taken over from fig. 5.

The comparison of hadron-hadron data with e^+e^- is basically more complicated. All contributions to the cross section, where the partons act coherently, should be excluded from the comparison. COOPER et al. (C2) discussed already 1975 the importance of leading particle effects. This is stressed again in the recent comparisons by BASILE et al. (B6). In practice, various procedures were applied to account for the leading particle effects or for the diffractive component in hadron-hadron interactions. Some recent results (B6-9, M2, C3) are shown in fig. 9 together with the e^+e^- curve. In conclusion, using the appropriate effective energy all data on the mean charged multiplicity follow within about one unit the same curve.

Sphericity

The axis of a multihadron system is usually not given a priori. Therefore, the above mentioned minimization procedure must be applied to obtain an axis and the sphericity with respect to this axis.

Neutrino experiments offer a unique way to compare experimentally the reconstructed sphericity axis $\vec{e}_S$ with the a priori known W-boson axis $\vec{e}_Q$ being the direction of the lepton momentum transfer. Fig. 10 shows that the average angle between these two axes decreases with increasing invariant mass of the hadron system. It is obvious that the true sphericity is considerably underestimated at low energies, if evaluated with respect to $\vec{e}_S$. Another commonly used quantity for measuring the jetlikeness of a multihadron system is the quantity thrust,

$T = \max_{\vec{e}_T} \frac{<|\vec{p}\,\vec{p}_T|>}{<|\vec{p}|>}$, formed from linear quantities only. At low energies the sphericity and the thrust axes differ systematically (fig. 10), but at PETRA energies they coincide within a few degrees.

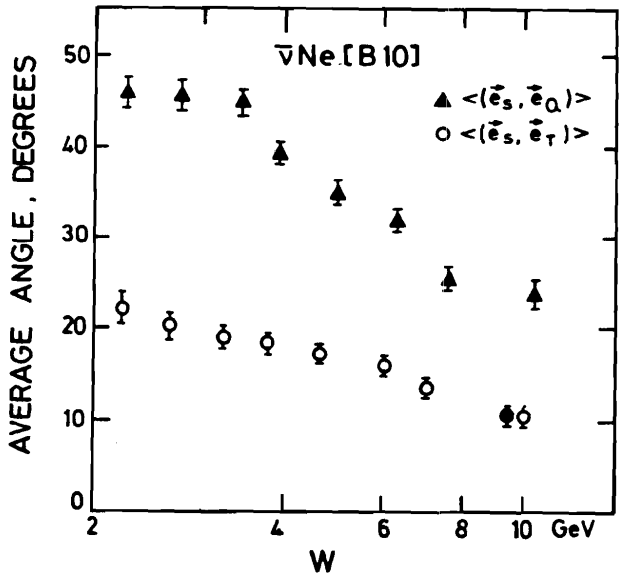

Fig. 10:

Measured average angles between various axes ($\vec{e}_Q$ is the current direction, $\vec{e}_S$ is the sphericity axis, $\vec{e}_T$ is the thrust axis). The full dot is a measurement from e^+e^- (F8).

The average sphericity measured in e^+e^- (W1) is shown as a function of the c.m. energy $\sqrt{s}$ in fig. 11 and compared in fig. 12 with some ℓN and hh data. The ISR low P_T jets (M2) give values systematically below the e^+e^- curve. Comparing the actual shape of the sphericity distribution with the e^+e^- distribution at the same energy, an access of events appears to be at low values of sphericity. This suggests an incomplete removal of the diffractive component.

In conclusion, all data on e^+e^-, ℓN and hh hard scattering agree approximately in the average multiplicity and the average sphericity provided the effective energy is used. The behaviour of low P_T proton-proton data seems to be different.

It makes sense to talk about jets in

- lepton-nucleon deep inelastic scattering for $\sqrt{s_{eff}} = W \gtrsim 6$ GeV
- e^+e^- scattering for $\sqrt{s_{eff}} = \sqrt{s} \gtrsim 12$ GeV

This choice ensures a pronounced jet structure. The high lower bound in e^+e^- is required in order to have a well defined axis.

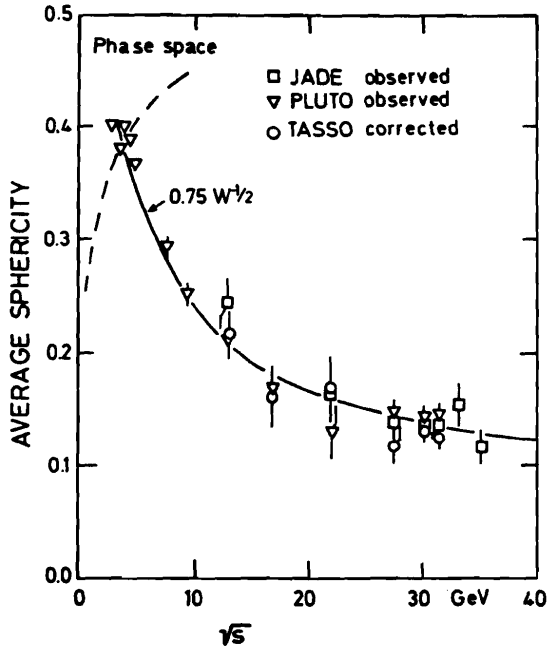

Fig. 11:

Average sphericity versus centre of mass energy for e^+e^--annihilation.

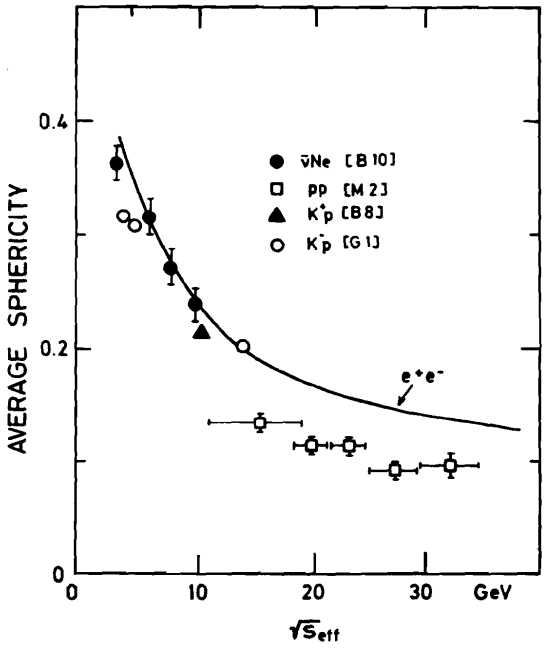

Fig. 12:

Same as fig. 11. Comparison with $\bar{\nu}$ data and with low P_T hadron-hadron data.

High p_T Jets in hh-Interactions

With the above considerations in mind the observability of high p_T jets in hadron-hadron interactions, mainly proton-proton, will be investigated.
The requirement $\sqrt{s_{eff}} > 12$ GeV for seeing jets without a priori axis translates into an inequality for the fractional momenta of the partons, which undergo the hard scattering:

$$\sqrt{x_1 x_2} > \frac{12 \text{ GeV}}{\sqrt{s}} = \begin{cases} 0.50 \text{ for SPS 300 GeV pp} \\ 0.19 \text{ for ISR 2x31 GeV pp} \end{cases}$$

So, an experiment aiming at the observation of high p_T jets is faced with two problems:

(i) overlap between the 2 high p_T and the 2 low p_T (spectator) jets

(ii) process extremely rare due to the shape of the proton structure functions.

The NA5 Experiment

The dedicated interest of this experiment (P3) is the study of inelastic hadron-hadron collisions by using an unbiased jet trigger. The main part of the experimental setup represents a fine grain calorimeter with large solid angle acceptance. In fact, there is full acceptance in azimuth and about $\pm 45^0$ around the polar centre of mass angle $\theta^* = 90^0$, leading to the central rapidity range of $|y| < 0.8$. Events were selected by requiring a large transverse energy $\Sigma(E_i)_T$.
Fig. 13 shows the cross sections versus transverse energy for three trigger conditions. If final states were dominated by pencillike high p_T jets the ratio between the 2π-trigger and the 1π-trigger should be about 2. The preliminary experimental result, however, is not a factor 2, but a factor 10-100! Surely, even at $\Sigma(E_i)_T > 10$ GeV,jets, if they are there, look far from being pencillike (fig. 10). The event structure would, however, according to Monte Carlo simulation, remain jetlike.

Since the theoretically expected 4 jet cross section is very small (cf. fig. 13), rare phenomena in low p_T physics, never investigated under these extreme conditions, become prominent. As a matter of fact, at pp topological cross sections as low as $10\mu b = \frac{1}{3000}\sigma_{inel}$ typical final states consist of 30 charged particles (fig. 14), inducing a substantial background. Indeed, the total charged multiplicity around $\Sigma|p_T| = 10$ GeV is high, much higher than the one expected for high p_T jets (fig. 15). One may speculate that the event configurations, accessible sofar up to $\Sigma|p_T| = 15 \text{ GeV} \approx \frac{2}{3}\sqrt{s}$, are due to multijet production.
It would be interesting to investigate quantitatively events corresponding to topologies selected in ISR experiments with high p_T single particle triggers.

In conclusion, unbiased calorimeter triggers are not suited to the study of high p_T jets at SPS energies.

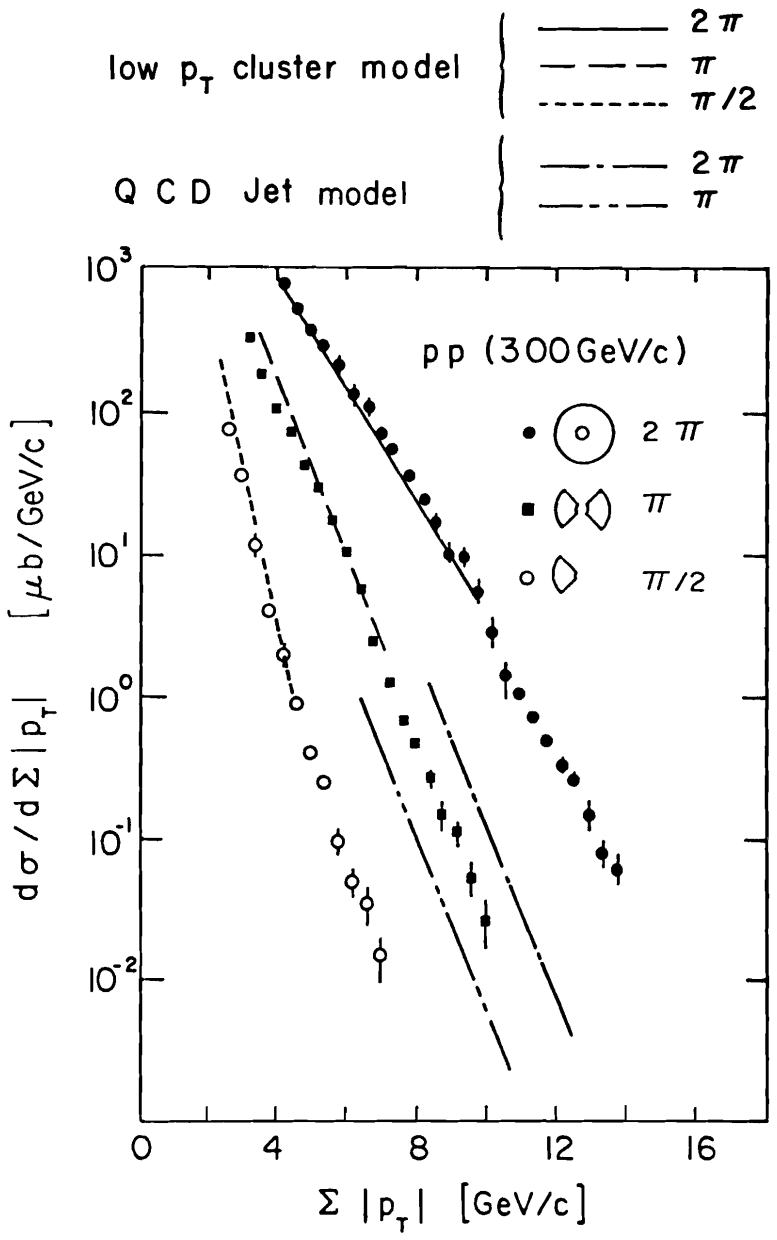

Fig. 13: Cross section versus transverse energy $\Sigma|p_T|$ measured for 3 trigger conditions. The comparison with the low p_T cluster model and the QCD 4 jet model are also shown.

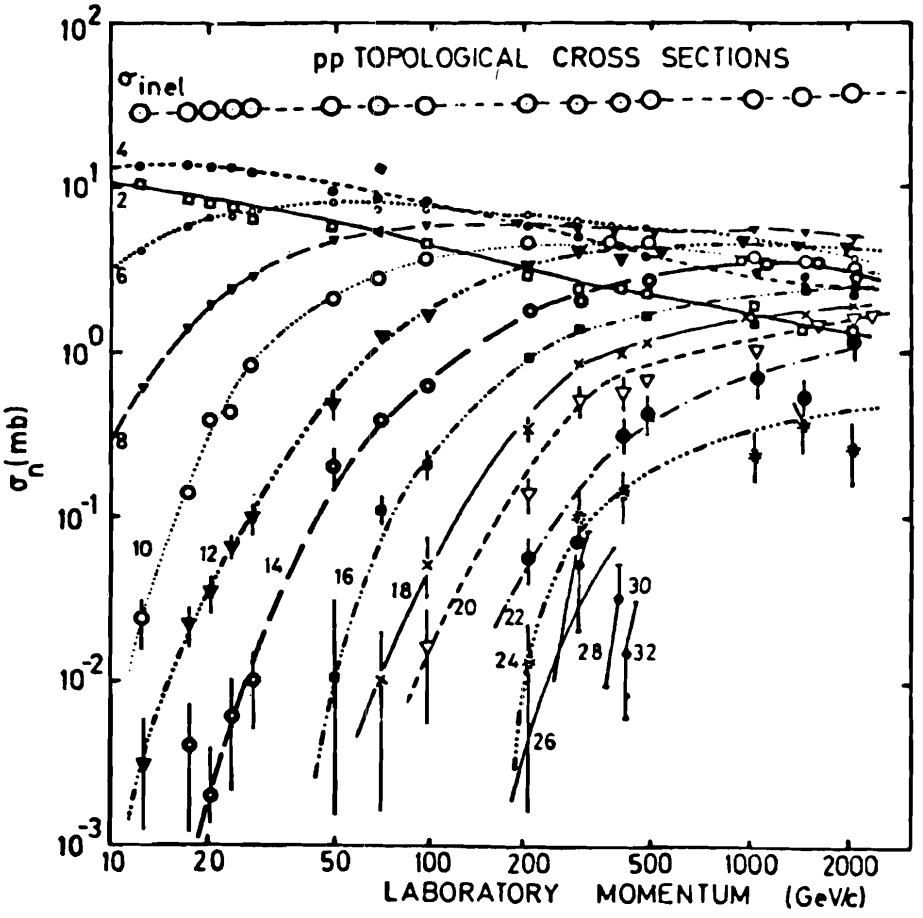

Fig. 14: The topological cross sections σ_n for pp → n charged particles versus laboratory momentum.

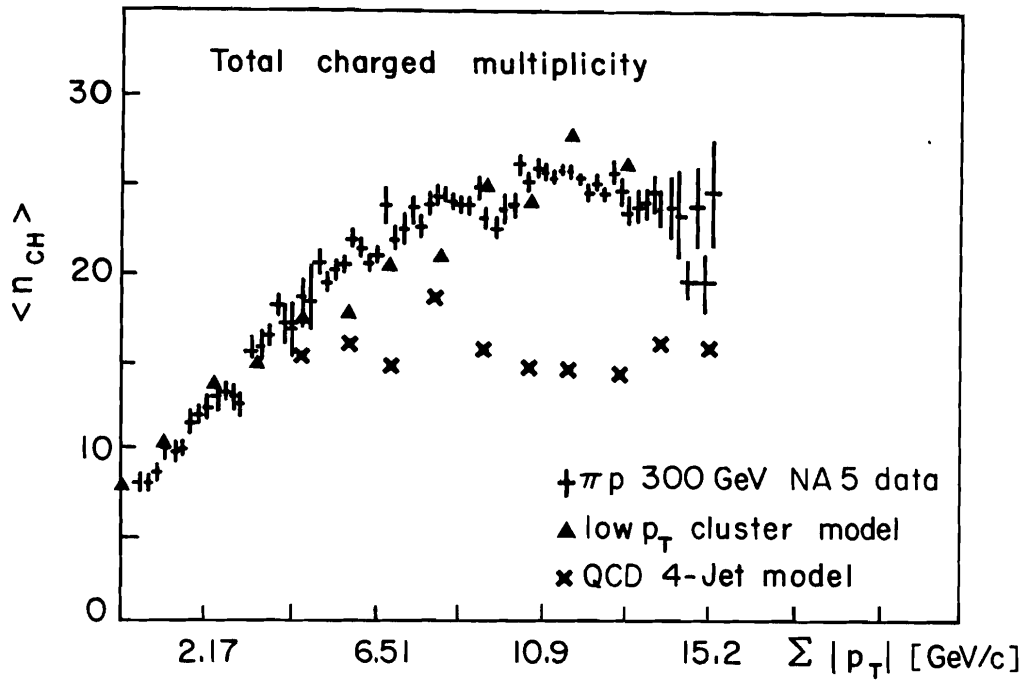

Fig. 15: The total charged particle multiplicity for πp collisions at 300 GeV/c as a function of the trigger threshold for the full calorimeter trigger.

The R-416-Experiment (A13)

In searching for high p_T jets the classical one particle trigger is applied. The trigger particle is selected at $\theta^* = 45^0$ with transverse momenta of 2, 4 and 6 GeV. For the following plots events with at least one secondary particle with more than 1 GeV/c transverse momentum were used.
Fig. 16 (F7) shows the rapidity for the trigger side (upper half) and the away side (lower half) distributions. The peaks of the secondaries at the trigger side are well pronounced around y = 0.9 for trigger $p_T > 4$ GeV/c. There is little background from the spectator jets. However, the away side jet appears to be very broad even at the highest trigger p_T. The reason for the broad shape can be understood. The quark giving rise to the trigger jet is fixed in angle by selection, whereas its partner in the hard subprocess has a sizeable momentum spread. Indeed, selecting the fastest away side particle in a fixed (note the bar in fig. 16b and c) rapidity interval the jet structure becomes prominent (F4). The jet moves, as it should, with the preselected rapidity interval. The width of the away jet is now similar to the width of the trigger jet.
It may be noted that due to the requirement of at least one secondary on the trigger side the trigger particle carries about 74% (F7) of the parton momentum (fig. 29). The away side jet is not biased.

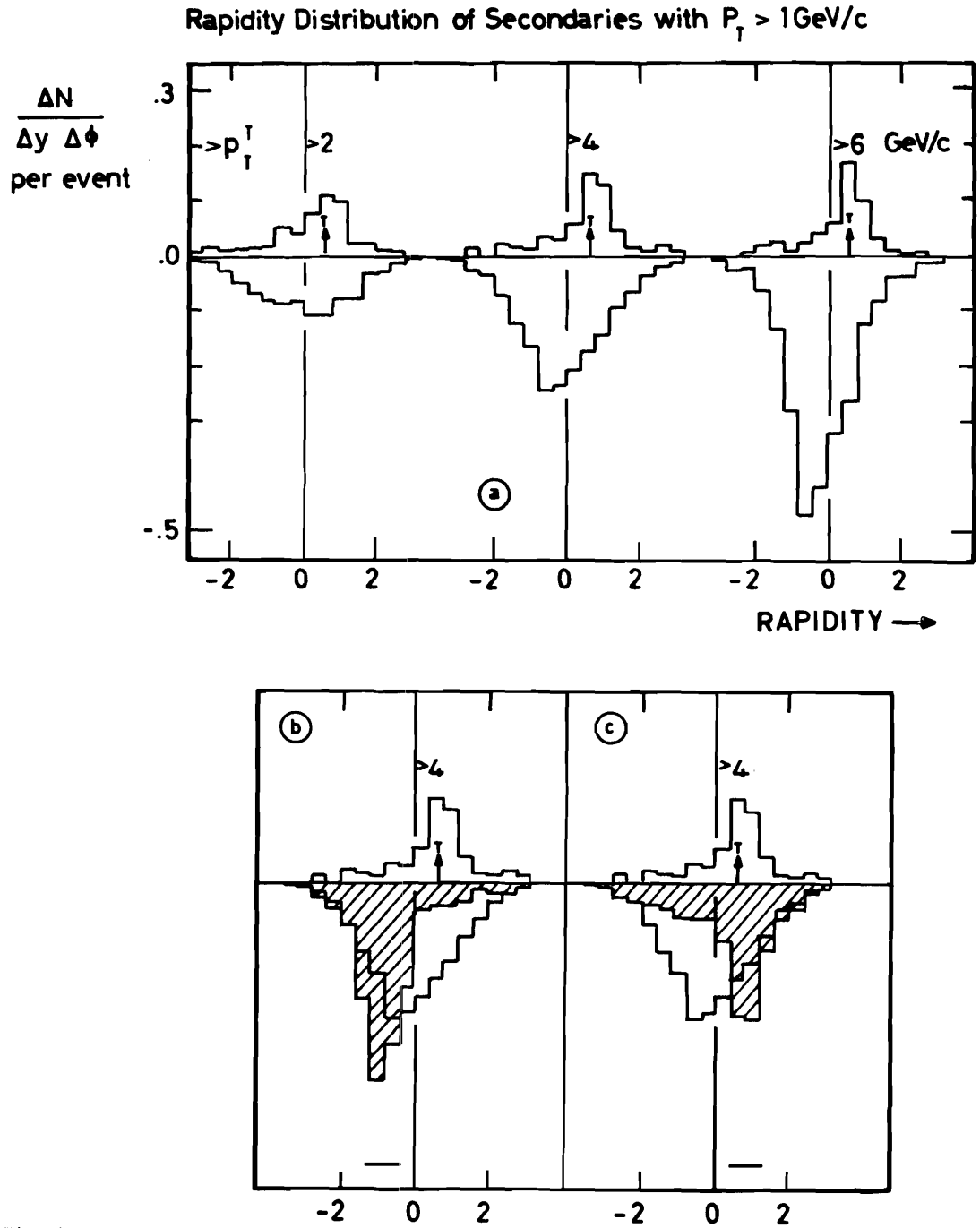

Fig. 16: Rapidity distribution of secondaries with p_T > 1 GeV/c on the trigger side (above 0) and away side (below 0). The trigger particle is indicated by an arrow, but not included. In (b) secondaries are marked in hatched if the fastest away side particle falls in the rapidity interval indicated by the bar. (c) as (b) but different rapidity interval.

III. PROPERTIES OF JETS

Origin of Jets

The phenomenon of jets is not restricted to strong interactions, but emerges also in electro-weak interactions provided the relevant processes are hard enough. Hard process is but another word for short distance process. The universality of jets must therefore be related with basic properties at the subnuclear level. Such a property is color. Sofar no colored objects were detected as free particles in nature (confinement). In the parton model the origin of jets may be seen in the separation of colored partons (S3). A perspicuous example is a neutrino proton interaction (fig. 4b), where the intermediate vector boson, being colorblind, sees only the flavour of the partons with the result that a colored current u-quark moves apart from an anticolored target uu-quark. The potential energy of the color force field between the separating colored objects gets transformed into uncolored mesons and baryons by the creation of quark-antiquark and diquark-anti-diquark pairs. The created $q\bar{q}$ pairs are "discoloring" the color force field and are so generating a jet. The details of this process are not yet understood and models for the fragmentation were built (F5, A4,P4). The parameters (F6) characterizing the cascade cannot be calculated within the model and are adjusted to experiment.
This discussion indicates two aspects: the short distance aspect, which includes the parton dynamics, and the long distance aspect, which includes the jet dynamics. The fact, that jets are witnessing of the underlying parton dynamics, makes them not only interesting objects, but also important tools. Leptons and photons as opposed to partons do not carry color and are thus escaping the short distance region without any hindrance.

Color Source Configurations

Jets reflect the original color source configuration. Fig. 17 illustrates a few examples within the color string picture (S3). Jets in electroweak interactions form dominantly collinear (fig. 17a,b,c), but sometimes also coplanar configurations (fig. 17d). This can be seen in fig. 18, where the mean squared transverse momentum of the forward and backward jets are plotted for various experiments as a function of the relevant centre of mass energy. The forward jet in lepton-nucleon scattering events consists of all hadrons with Feynman $x_F > 0$ in the hadron centre of mass frame. Jets in e^+e^- events do not have an a priori orientation and are ordered by calling forward the jet with the higher invariant mass. This procedure entails a well understood selection bias disappearing with increasing jet multiplicity. Quarks or antiquarks with hard gluon radiation are almost always contributing to the jet called forward. It is then seen that forward jets are increasingly more broadened with increasing energy, whereas the backward jets show no or very little variation. A small fraction of the high energy PETRA e^+e^--jets exhibit a three jet structure (P5,B11), seen now also at PEP (H5). Coplanar configurations in ℓN scattering, similar to fig. 17d for e^+e^-, are recognizable also in angular energy flow diagrams (A6,B14). There are also indications of jet broadening in high p_T ISR-jets (A14).

The observed jet broadening is well described by QCD in first (H6,A4) or second order (A7) plus standard fragmentation. There is, however, a point of particular importance. In collinear confi-

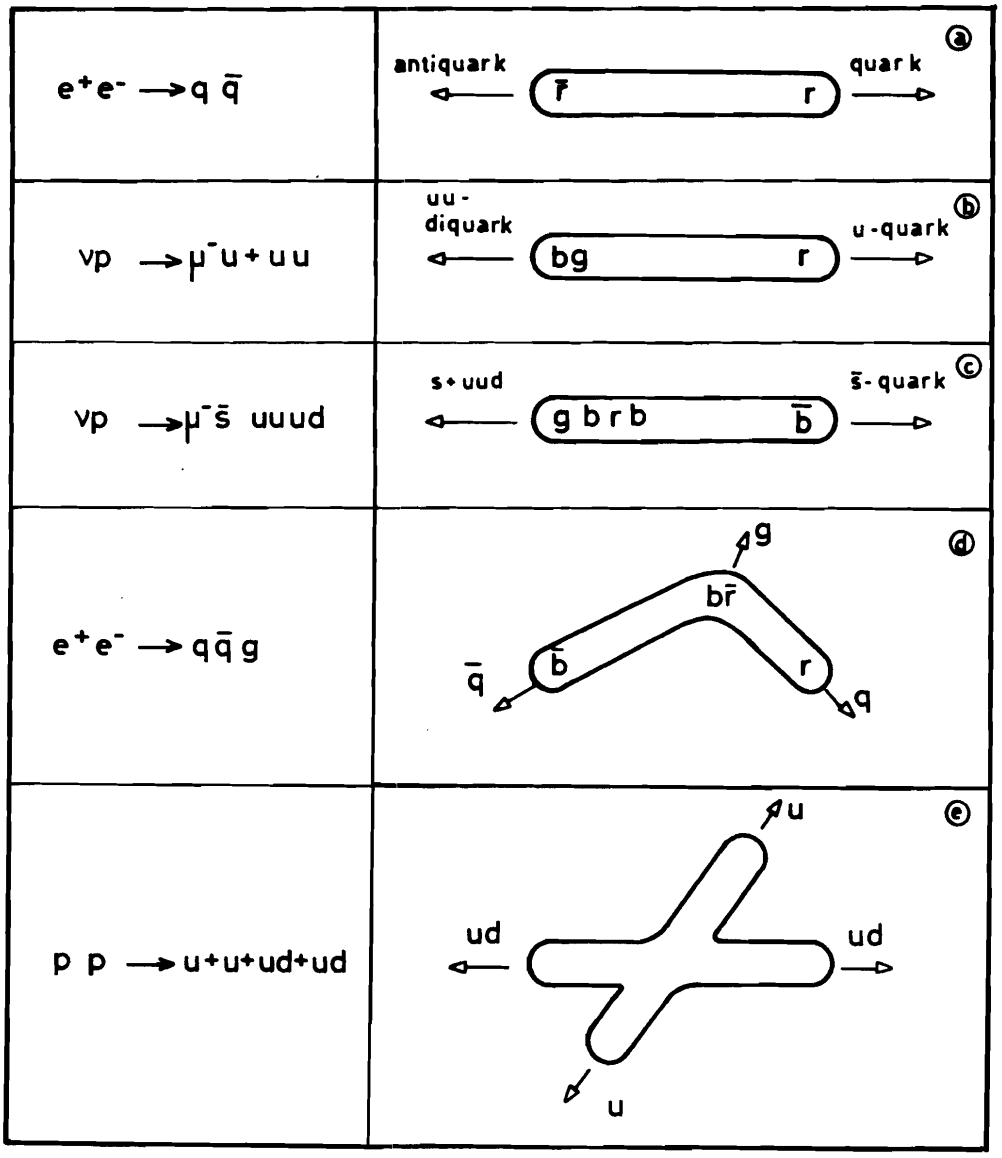

Fig. 17: Various color source configurations.

gurations. As sketched in fig. 19 it matters whether the fragmentation proceeds along the original parton axes or along the "strings" (spanned between the color-anticolor pairs (fig. 17d)). The predictions will be systematically different. The JADE collaboration (B15) has confronted their data with 2 models based on first order QCD (A4,H6), differing in the choice of the fragmentation axes. The string picture is clearly preferred. A recent comparison is presented in fig. 20 (P6), where all data, not only a subsample of three jet events, are shown together with the LUND ("string") model (A4) and a parton fragmentation model with QCD in second order (A7).
There are other models (P4) which explain coplanar configurations by the possibility of jet branching. A clear distinction to the above mentioned models is the absence of gluon jets.

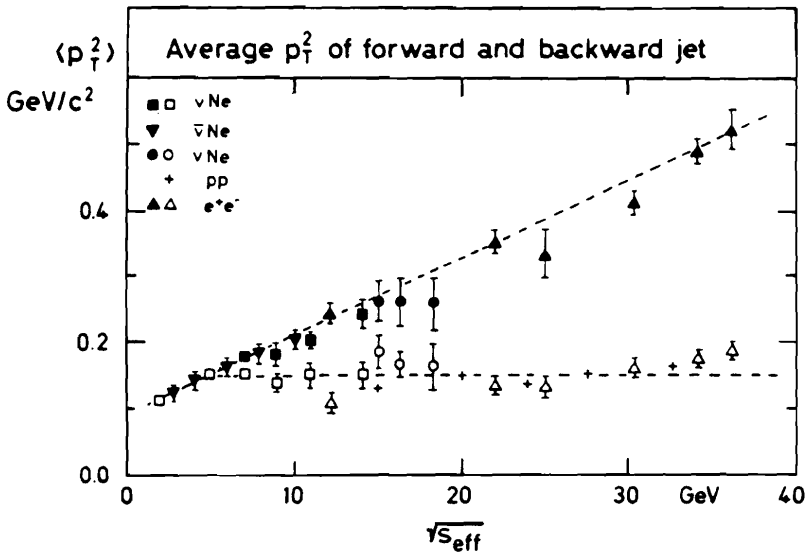

Fig. 18: Average p_T^2 of multihadron systems separately for forward (full symbol) and backward (open symbol) jets in the overall centre of mass frame. The dotted lines are not fits, but intended to guide the eye. The data included are taken from D1 (■□), B10 (▼ only forward), B14 (●○), M2 (+ low p_T jets), M6 (▲ △).

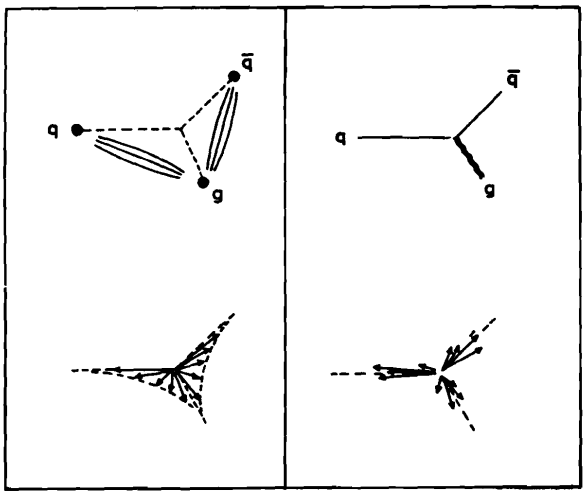

Fig. 19: Sketch of 2 fragmentation schemes in $q\bar{q}g$ events.

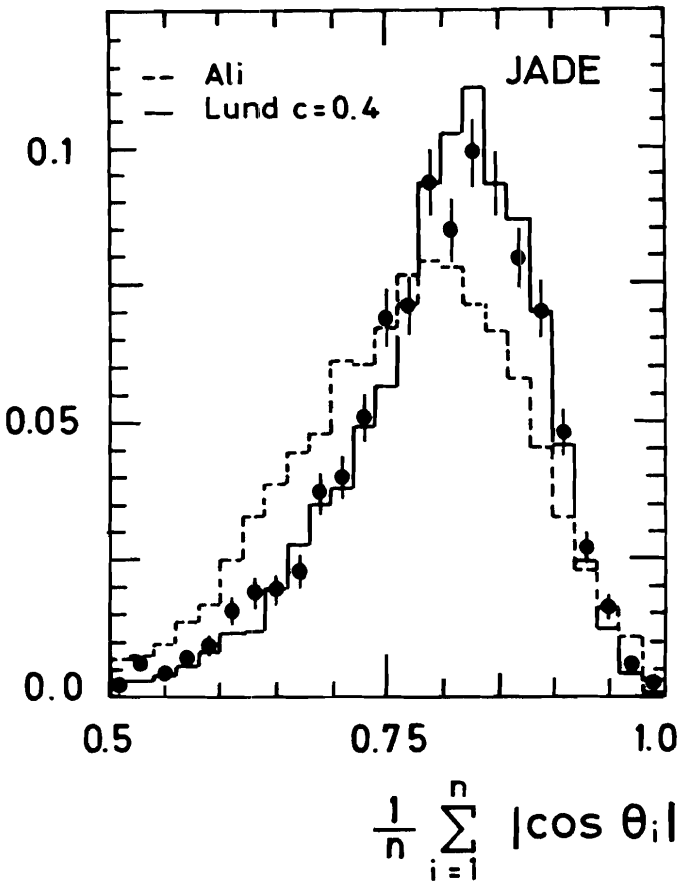

Fig. 20: The average cosine distribution compared to two models differing in the choice of the fragmentation axes. θ_i is the angle of the i-th hadron with respect to the sphericity axis.

Quark Jets

Jets in e^+e^- interactions behave as if induced by a quark-antiquark pair. The jet angular distribution should be $1 + \alpha\cos^2\theta$ with $\alpha = 1$, if spin 1/2 quarks are their origin. Indeed, the measurement gives $\alpha = 1.00 \pm 0.16$ (B11). Further evidence comes from the observation of a long range charge correlation (B13). Neutrino resp. antineutrinos current jets are induced by quarks of a priori known flavor, namely u resp. d (provided BJORKEN-x is not too small). The weighted charge distributions of current jets in νN and $\bar{\nu}N$ (B10), shown in fig. 21, agree well with the prediction of the FIELD-FEYNMAN model (F5). The energy dependence of the net charge cannot be reproduced by a model without quark fragmentation (B10). The FIELD-FEYNMAN model (F5) predicts such charge correlations, however they turn out to be stronger than experimentally observed (B12).

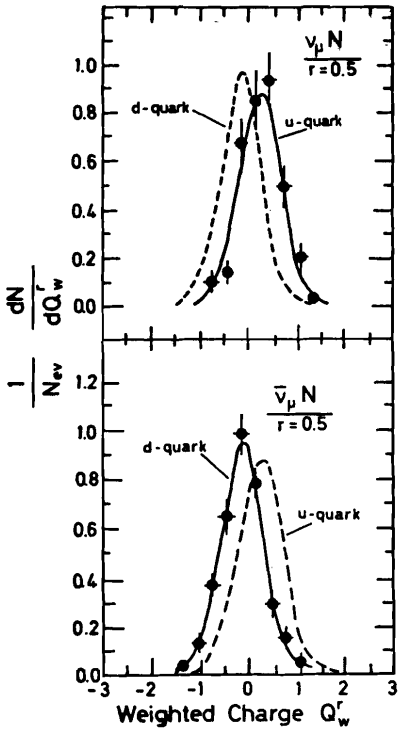

Fig. 21: The measured weighted charge distribution in νN and $\bar{\nu} N$ together with the prediction of the FIELD-FEYNMAN model.

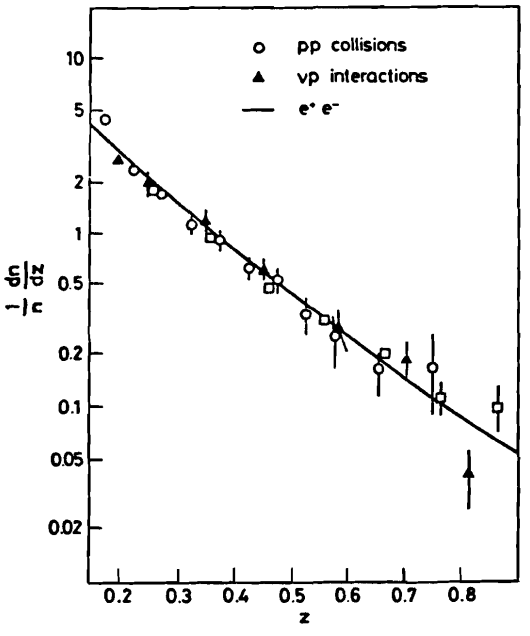

Fig. 22: Comparison of fragmentation in charged hadrons.

Extensive studies of quark fragmentation were carried out, mainly into charged hadrons (S9,R1,W1). Fig. 22 (C3) shows the fragmentation in charged particles of high p_T ($p_T > 5$ GeV/c) ISR data compared with νp and e^+e^-. It is not trivial to determine the fractional momentum z_i of each hadron in a high p_T jet, since ideally one would have to know the total jet momentum in the centre of mass system of the hard scattering process.
Recently more data on K^0 production (G2,B16,B17,H5,M3) in jets was published. The data agree in the shape of the FEYNMAN-x distribution with the $\pi^\pm$ data, the same holds for the p_T- distribution, which exhibits broadening (H5). The comparison of the data with model calculations controls the production rate of $s\bar{s}$-pairs in the fragmentation cascade, usually assumed to be 20% (F5). Various recent analyses prefer a smaller value (A12,B17,M3).
Sofar little data exists on vector meson production. The fraction of produced vector mesons compared to pseudoscalar mesons is known to be high indirectly from the low $\langle p_T^2 \rangle$ of pions and from the overall multiplicity. The ρ^0-mesons observed in νp (A5) have $\langle p_T^2 \rangle = (0.26 \pm 0.06)$ GeV/c^2 typical for first rank particles (F5).

As a further comparison with low p_T hadron-hadron interactions the p_T^2 distribution of K^+p is shown in fig. 23 together with e^+e^- data at similar energy (B8). The indicated model curves reproduce the data well.
The fragmentation functions of c- and b-quarks are rather poorly known.

Diquark Jets

Such jets are observed as the spectator jets in deep inelastic lepton-nucleon and hadron-hadron scattering. Diquark fragmentation is much less studied than quark fragmentation, experimentally as well as theoretically (S5). To some extent a diquark (fig. 17b) can be treated as an antiquark ($3 \times 3 = 6 + \bar{3}$). However, the very fact that a diquark is the simplest colored multiparticle system raises new challenging questions. For instance: how does a diquark become a baryon? what is the effect of the spatial extension of the diquark?
Diquark jets and quark jets are different. Fig. 8 shows that the average multiplicity of target (diquark) fragments in $\bar{\nu}D_2$ interactions is much smaller than the one of current (d-quark) fragments. The rapidity distribution of the net charge (fig. 24) demonstrates that, in the centre of mass system of the hadronic final state, it makes sense to distinguish forward and backward fragments provided the effective energy is big enough (S6). A striking example of the flavor-dependence of diquark jets is provided by an ISR experiment (F7), where a prominent Δ^{++} resonance is present in the forward diquark jet flavor defined by a high p_T forward π^- ($= \bar{u}d$) trigger. The Δ^{++} is absent if instead a π^+ trigger is used (fig. 25). In a νp experiment fragmentation into π^- is measured both in forward and backward direction and much different slopes are observed as expected (S4). Further studies of diquark jets could be made in Drell-Yan events.

Gluon Jets

Coplanar configurations as a result of jet broadening, observed in many experiments (fig. 18), are recognized to be in part three-jet structures at the highest PETRA energies (P5), also reported at this conference by PEP (H5). Many efforts went and still go in an unambiguous proof that one of the three jets is due to a gluon. The difficulty lies in the fact, that the differences between a gluon and a quark jet get washed out, when they fragment.

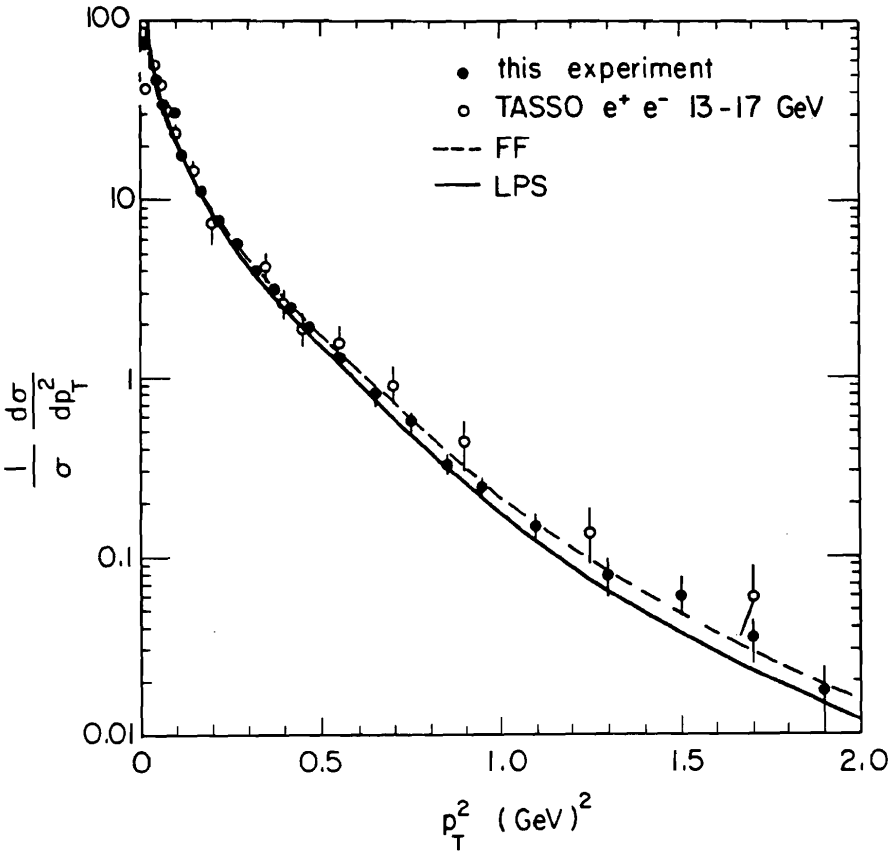

Fig. 23: Distribution of the mean transverse momentum squared of low p_T jets in K^+p (B8) with e^+e^-.

Angular and momentum analysis of the 3 jet events exclude the hypothesis of a scalar gluon, but agree well with a vector gluon (B11,H5). The comparison of gluon model predictions with 3-jet data suggest that gluons fragment differently from quarks (B15,B11). Reported to this conference are further indications that the lowest energy jet, which is most likely the gluon jet, has a larger $\langle p_T \rangle$ than the other two (quark and antiquark) jets in and out of the event plane (B11). The study of the neutral energy fraction in 3-jet events does, however, not give any hint on the charge 0 of the gluon (B19). Also, the PEP-MkII (H5) group found the shape in p_T^2 for the fast jet less steep than for the slow jet, contrary to expectation.

A different handle on gluons is offered by ISR experiments in studying high p_T photon events (M4) or events selected by high p_T K^--triggers (F7).

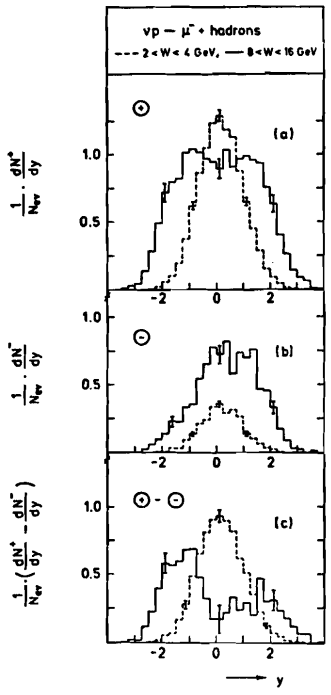

Fig. 24: Positive, negative and net charge distributions versus rapidity for 2 intervals of the total hadron invariant mass.

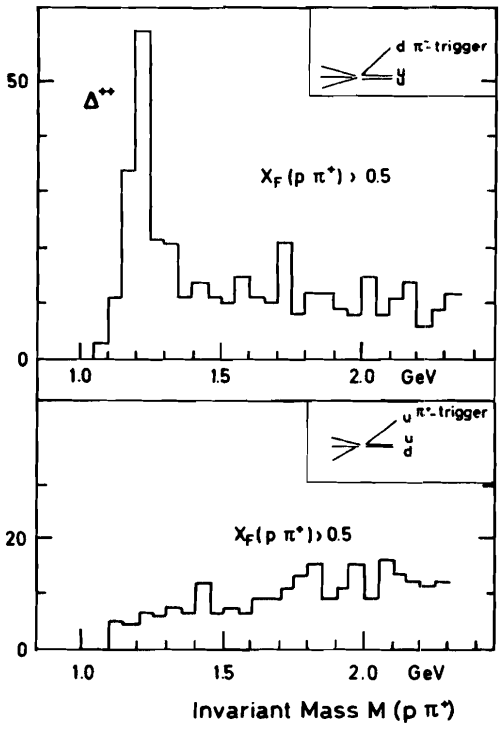

Fig. 25: $p\pi^+$ invariant mass distributio in forward spectator jets give a forward π^- and π^+ trigger (see sketch).

Baryon Production

In the jet fragmentation process little attention has been paid to the production of baryon-antibaryon pairs. Recent experiments, however, show that the baryonic fraction in jets is not negligible. This new feature complicates the fragmentation process, but may offer on the other hand a deeper insight.
In table 2 rates on proton and lambda production , measured in e^+e^- and ℓN experiments are listed.

Experiment	Energy $\sqrt{s_{eff}}$ in GeV	$\frac{1}{2}\,\#(p+\bar{p})$ / event	measured quantity	$\frac{1}{2}\,\#(\Lambda+\bar{\Lambda})$ / event	measured quantity	Ref.
JADE	34	0.20 ± 0.02	$\bar{p}$	0.063 ± 0.017	$\bar{\Lambda}$	B18
TASSO	30	> 0.2	$p+\bar{p}$	0.16 ± 0.05	$\Lambda+\bar{\Lambda}$	B16
PEP-MKII		> 0.2	$p+p$			H5
		# p forward / event		# Λ forward / event		
EMC	8-17	≈ 0.1	$p,\bar{p}$	_	-	A9
BEBC	5	_		0.025 ± 0.004	Λ	G2

The JADE e^+e^- data on $\bar{p}$ production were obtained at low momenta only and then extrapolated (A8). The MARK II measurements (H5) agree with all PETRA data up to 1.5 GeV/c, between 1.5 and 2.0 GeV/c they show a different trend. No attempt has been made to extrapolate the data. Also the rate of 1 and 2 baryon-antibaryon pairs in the MARK II experiments seems to be much bigger than expected from the PETRA experiments on the basis of their single baryon or antibaryon rates. The data on $\bar{\Lambda}$ production observed by JADE (B18) agree with $\frac{1}{2}(\Lambda+\bar{\Lambda})$ observed by TASSO (B16) and MARK II (H5), (fig. 26). The difference in rate given in table 2 may be due to the extrapolation procedure (A8). It is amazing to note that the Feynman-x distributions for Λ or $\bar{\Lambda}$ and $\pi^{\pm}$ agree in shape within errors provided $x > 0.2$ (F3) (fig. 26). Is there an indication for a similar production mechanism? The LUND group (A8) has extended its jet program based on string fragmentation. They introduced as a new ingredient the creation of diquark-antidiquark pairs, which give rise to baryons and antibaryons in much the same way as quark-antiquark pairs give rise to mesons. The application to the PETRA data shows good agreement with p production and slight underestimation of Λ production. Other attempts were made in ref. M5 and S10. The EMC Collaboration has observed forward produced p and $\bar{p}$ in deep inelastic muon proton scattering (A9) (fig. 26). The LUND model (A10) describes well their z-distribution. If applied to the forward produced Λ in the BEBC νp experiment (G2), it seems again to underestimate the data. Only a small fraction of the forward baryons, $x_F > 0$, are spilling over from the target fragments.
Only little data exists on baryon production in hadron-hadron collisions. The ratios $\#p/\#\pi^+$ and $\#\bar{p}/\#\pi^-$ are shown in fig. 27 versus $x_T = \frac{2p_T}{\sqrt{s}}$ (A11). It would be interesting to investigate the correlation of baryons in the spectator jets given a high p_T baryon or antibaryon.

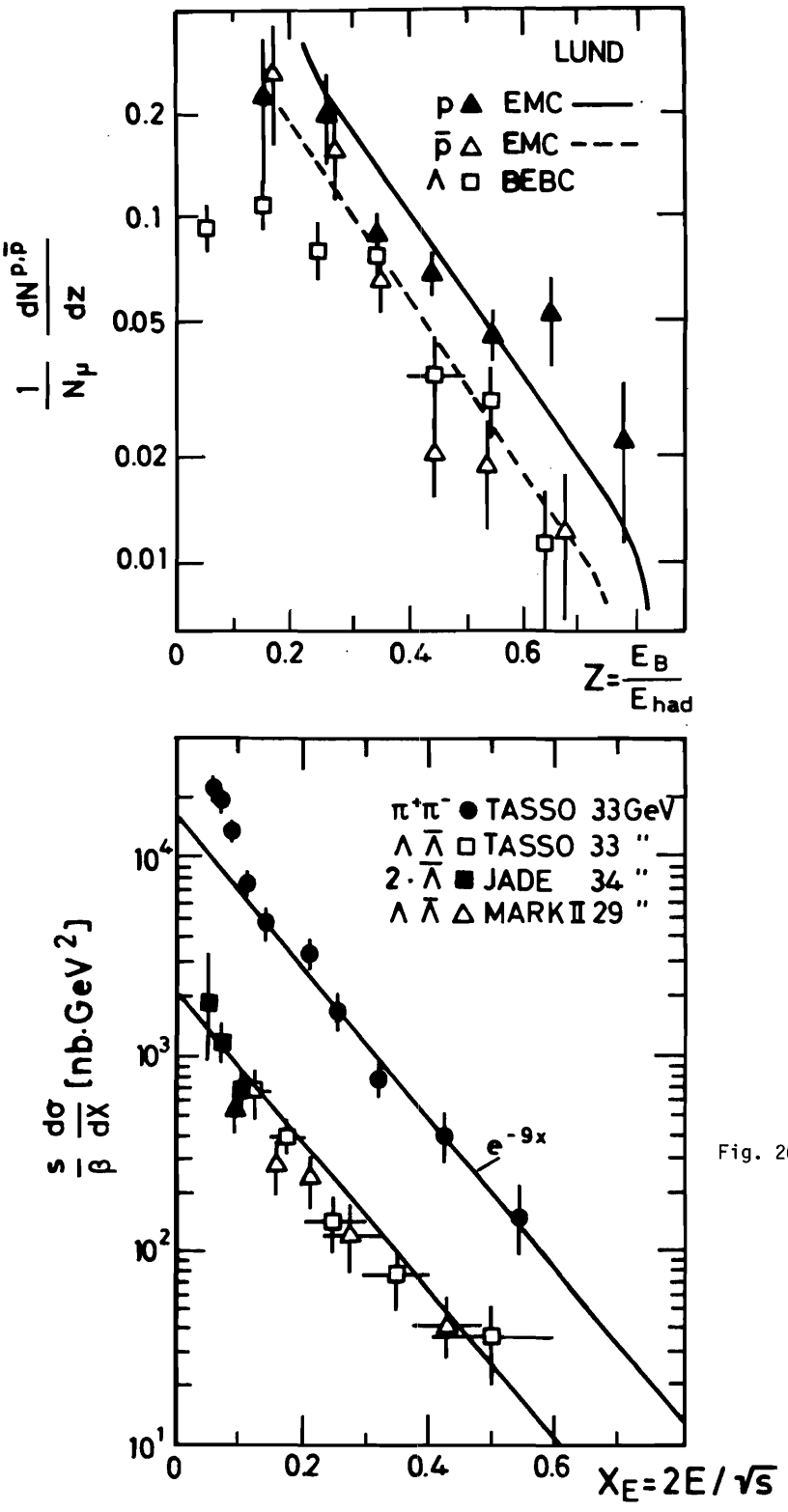

Fig. 26: Baryon-antibaryon production. The curve e^{-9x} is an eye-ball fit to the $\pi^{\pm}$ data.

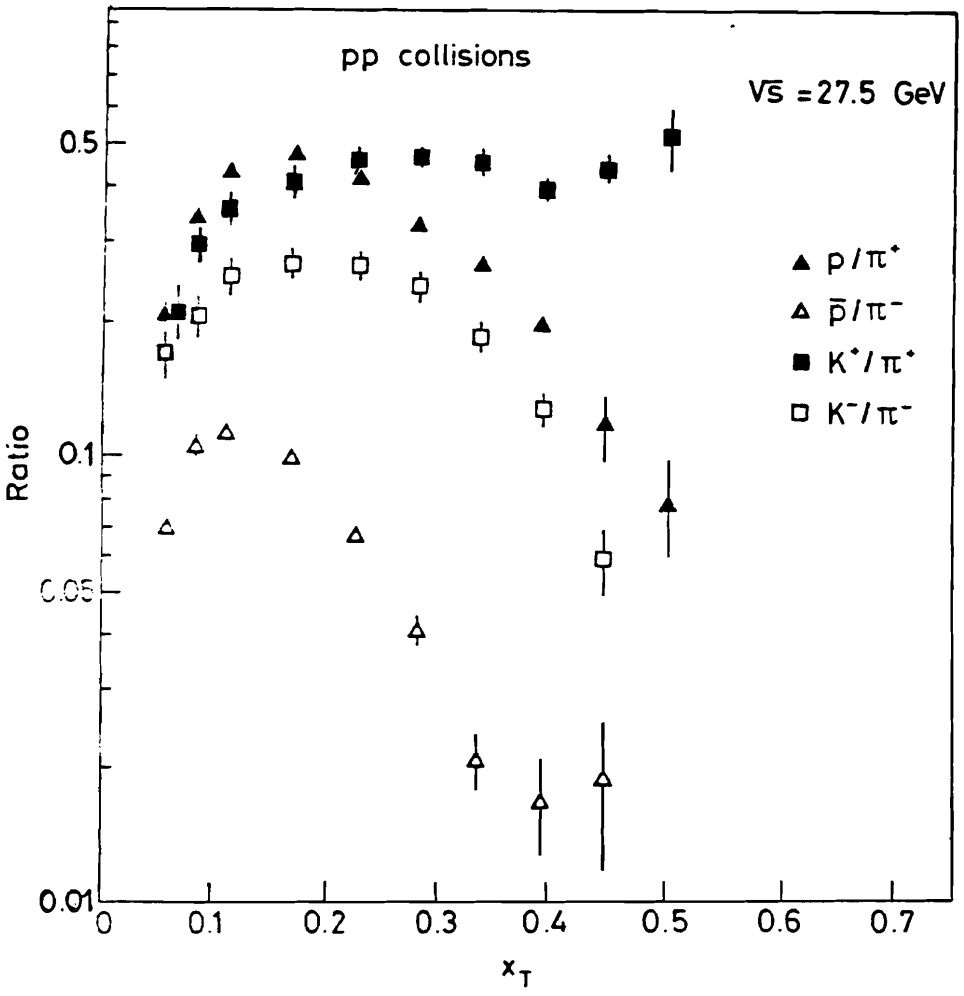

Fig. 27: Inclusive production rates in pp collisions as a function of $x_T = \frac{2p_T}{\sqrt{s}}$.

In conclusion, jets have a sizeable baryonic component, which increases roughly in proportion to the total multiplicity. At present energies the rate of any kind of baryon-antibaryon pairs per event in ℓN experiments amounts to about 20%, in e^+e^- (PETRA) experiments to about 50%. The data raise questions, such as:

- are baryon pairs produced locally;
- is the production mechanism related to diquarks;
- why is the slope of the x dependence so similar for baryons and mesons?

Scaling Violation

Two experimental groups have presented at this conference evidence for scaling violations in fragmentation functions. The process $e^+e^- \to h^\pm$ + anything was studied using the MARK II detector both at SPEAR and PEP (H5) such that systematic errors could be kept small. It turns out (fig. 28), that $s\frac{d\sigma}{dx}$ increases with s for small x ($x < 0.2$), but decreases with s for big x ($x > 0.4$). This implies a fragmentation function $D^h(x,s)$. Its s-dependence is predicted by QCD. The high energy data have been compared (H5) with the TASSO data and agree. The TASSO data alone, although spanning the range from 13 till 36 GeV, do not yet allow to establish scaling violations (W1). The low energy data play therefore a decisive role. Phase space effects and effects due to charm and beauty thresholds may have some influence. It would be nice to demonstrate scale violations in the range 13 to 35 GeV alone.

The EMC-group (M3) has observed in $\mu p \to \mu + h^\pm$ + anything that the fragmentation function for fixed BJORKEN-x and $z = E_h/(\Sigma E)_{Had}$ depends nontrivially upon Q^2, i.e. $D^h(z, x, Q^2)$. The measurements extend up to $Q^2 = 400\ GeV^2$.

Several Neutrino groups have analysed their data in terms of single and double moments of fragmentation functions (S9,R1). In these experiments, covering a smaller range in Q^2 than EMC, the observed scaling violations are mainly due to events with low W^2.

Clearly, scaling violating in jet fragmentation is an important phenomenon. Such effects are expected in QCD, but also higher twist contributions may play a role. More work will be needed to consolidate the present results.

IV APPLICATION OF JETS

High p_T jets resulting from hard scattering in hadron-hadron interactions give information about the underlying elementary process (F7). At ISR energies high p_T jets arise mainly from qq and qg scattering. Jets selected by a high p_T trigger particle suppress strongly contributions from partons belonging to the sea of the proton. The nature of the trigger particle is closely correlated to the parton flavor, e.g. a π^+-trigger selects mainly u-jets, a π^--trigger d-jets and a K^--trigger gluon-jets (F7). So, the properties of the high p_T trigger- and away side jets would allow in principle to isolate individual parton-parton processes. In particular, qg-interactions are sensitive to the triple gluon vertex.

The following figures serve to illustrate some of the above considerations. The longitudinal momentum fraction $x = p_{||}/p_{trig}$ with respect to the momentum of two trigger particles, namely π^+ and K^-, are displayed in figs. 29, 30 for secondaries with the same and opposite charge as the trigger particle. Monte Carlo calculations with FIELD-FEYNMAN fragmentation and $E_{\pi^+}/E_u = 0.74$ reproduce the observed distributions (fig. 29). In the case of the K^--trigger the shapes of the distributions in fig. 30 cannot be fitted, if a quark jet fragmentation is assumed. At high transverse momenta a K^- being composed of $\bar{u}s$, which are not available in the proton as valence quarks, is most likely due to a gluon. Fig. 30 shows indeed a much softer fragmentation. The properties of the away side jets in events selected by a π^+ trigger should allow to disentangle uq from ug interactions. The charge ratio in away side jets is plotted versus $x_E = \frac{p}{p_{trig}}$ for negative and positive rapidities

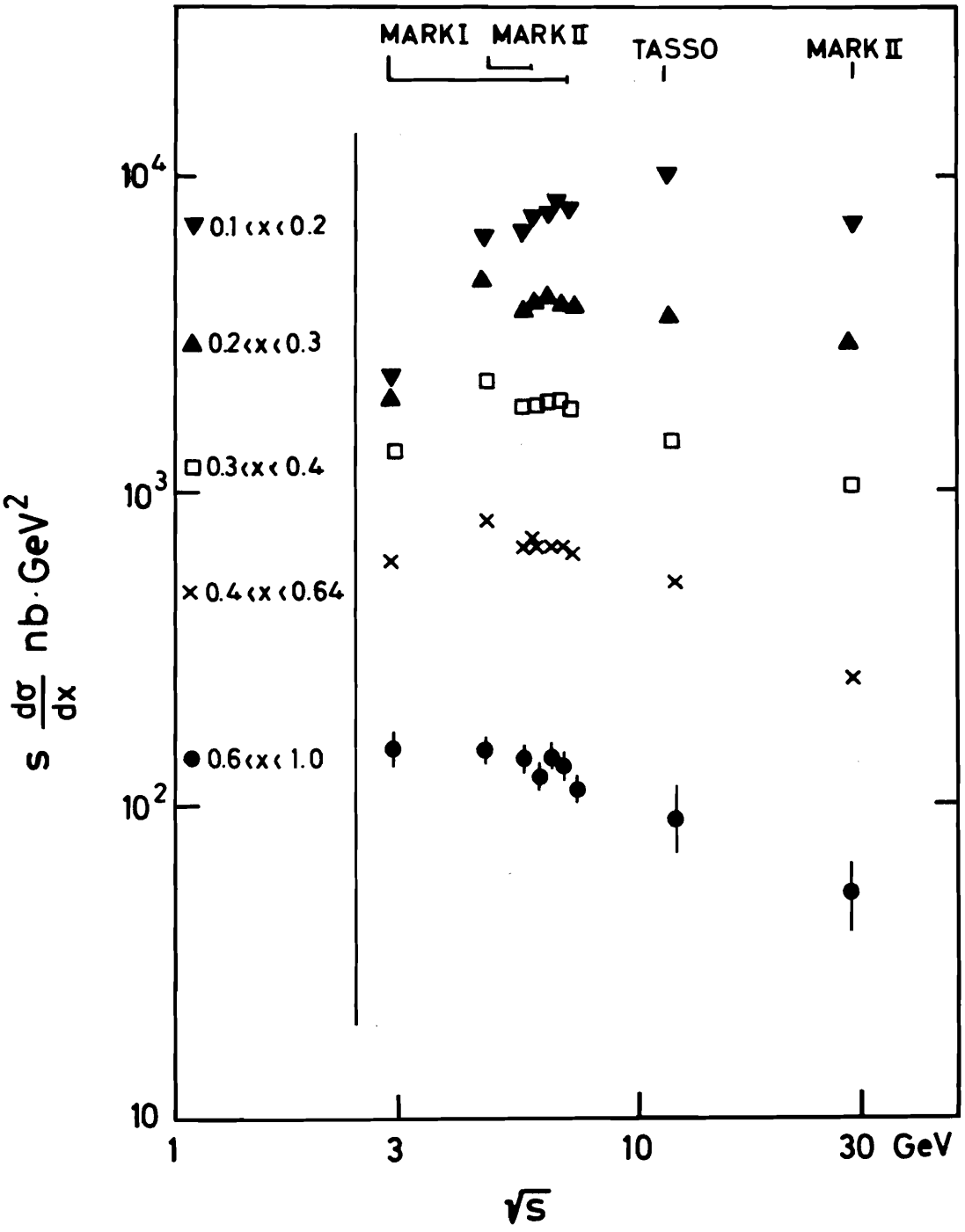

Fig. 28: Scaling violation in e^+e^- annihilation (H5).

Fig. 29: x-distributions of secondaries of both charges for π^+ triggers.

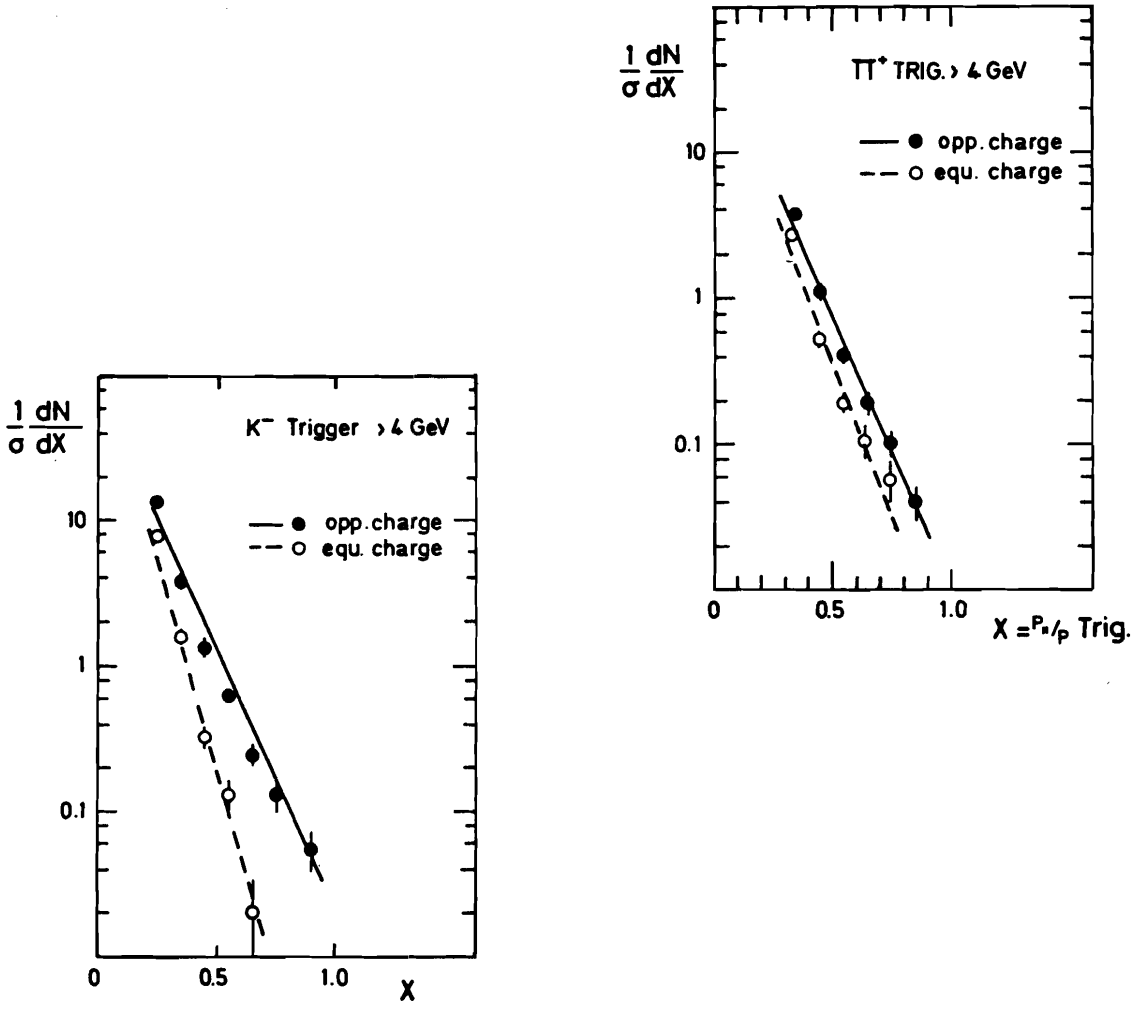

Fig. 30: Same as fig. 29 but for K^- triggers.

in fig. 31. The configurations are shown in fig. 16b and c. Events corresponding to fig. 16b require two roughly equally fast quarks, whereas configuration c arises from the interaction of a fast quark, giving rise to the trigger particle, with a somewhat slower parton, i.e. qq or qg. As expected, the charge ratio for away side jets with negative rapidity increases for high x_E to about 2 being the ratio of u and d quarks in the proton. On the contrary, for away side jets with positive rapidity the charge ratio is sizeably reduced. This is expected, if also jets induced by partons with charge zero would contribute.
These promissing analyses of the R-416-group are carried further.

Another area, where jets probe the underlying parton dynamics, are the three jet events in high energy e^+e^- interactions. They are interpreted in the framework of QCD and allow to measure the strong coupling constant (S8).

Finally, by studying the jet opposite to high p_T photons in pp (or $\pi^{\pm}p$) collisions the inverse QCD COMPTON process $qg \to q\gamma$ can be tested (M4, Z1).

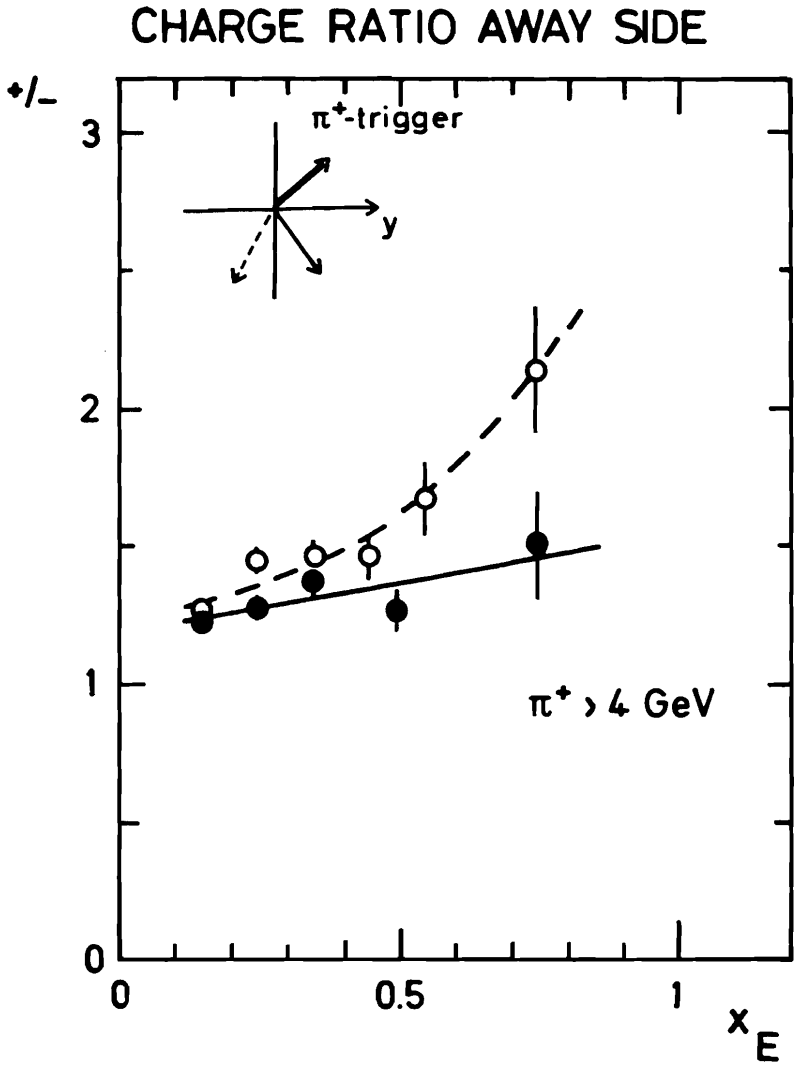

Fig. 31: Charge ratio as a function of x_E for π^+ triggers in 2 away side intervals (open symbols refer to y<0, full symbols to y>0).

V. OUTLOOK

Jet physics is still in a phenomenological stage. The originally simple description in terms of a scaling quark cascade proved to be only an approximation. The observation of copious baryon antibaryon production in jets asks for a more detailed description of the fragmentation process. Jet fragmentation in coplanar configurations depends upon the choice of the fragmentation directions. The observed violations are an important achievement.
Further studies are needed to establish the nature of gluon jets. Multiparton systems and their fragmentation are a logical continuation towards higher complexity. Their understanding is a prerequisite for a unified description of low and high p_T phenomena.

Progress in understanding jets improves the understanding of the parton dynamics. The present knowledge will very soon be submitted to a stringent test, when the CERN $\bar{p}p$ collider comes into operation.

Acknowledgement

It is a pleasure to thank Prof. E. Lohrmann for many discussions and for reading the manuscript. I have benefitted a lot from discussions with Dr. H.G. Fischer. For help and information for the preparation of this talk I am indebted to Drs. P. Bosetti, R. Eichler, R. Felst, P. Mättig, H. Montgomery, W.Ochs, R. Orawa, C. Peyrou, A. Petersen, K. Pretzl, B. Saitta, T. Walsh and to my scientific secretaries Drs. D. Cords and N. Wermes. I wish to acknowledge the careful typing by Mrs. S. Platz and drawing by Miss Kauffner.

LITERATURE

A

1) E. Albini et al., Nuovo Cim. 32A (1976) 101

2) P. Allen et al., Nucl. Phys. B181 (1981) 385

3) V.V. Ammosov et al., Quark jets from $\bar{\nu}$ Interactions II, IHEP preprint 81-94

4) B. Anderson et al., Phys. Lett. 94B (1980) 211

5) P. Allen et al., Inclusive production of ρ^0 in νp charged current interactions, CERN-EP/81-93

6) J.J. Aubert et al., (EMC), Evidence for planar events and a forward double jet structure in deep inelastic muon scattering, contr. paper 180 submitted to this conference, CERN-EP/81-10

7) A. Ali et al., Phys. Lett. 93B (1980) 155

8) B. Anderson et al., Contr. paper 59, LU-TP 81-3 (LUND preprint)

9) J.J. Aubert et al. (EMC), Contr. paper 179, CERN-EP/81-53

10) B. Anderson et al., Contr. paper 62

11) D. Antreasyan et al., Phys. Rev. Lett. 38 (1977) 115; Phys. Rev. D9 (1979) 764

12) V.V. Ammosov, Measurement of SU(3) symmetry violation in the quark jet, FERMILAB-Pub-80/31-EXP

13) Ames-CERN-Dortmund-Heidelberg-Warshaw Collaboration, ISR-Experiment R 416

14) A.L.S. Angelis et al., Phys. Lett. 105B (1981) 233

B

1) J.D. Bjorken, Rendiconti della Scuola Internazionale di Fisica ≫ Enrico Fermi ≪, Varenna 1967, Current Algebra at Small Distances, p. 55, Akad. Press 1968 *

2) " , Phys. Rev. 179 (1969) 1547

3) " and Paschos, Phys. Rev. 185 (1969) 1975

4) " and Brodsky, Phys. Rev. D1 (1970) 1416

5) S. Barlag et al., Charged hadron multiplicities in high energy $\bar{\nu}n$ and $\bar{\nu}p$ interactions, Contr. paper, submitted to this conference.

6) M. Basile et al., Phys. Lett. 95B (1980) 311; Phys. Lett. 92B (1980) 367

7) D. Brick et al., Phys. Lett. 103B (1981) 241

8) M. Barth et al., Jet like properties of multiparticle systems produced in K^+p interactions at 70 GeV/c, CERN-EP/81-44

9) M. Bardadin-Otwinowska et al., charged multiplicities of hadrons in hadronic and leptonic reactions, Contr. paper 176 submitted to this conference.

10) J.P. Berge et al., Quark jets from $\bar{\nu}$ interactions I, FERMILAB-Pub-80/62-EXP (Nucl. Phys. B) and III, FERMILAB-Pub-81/30-EXP

11) W. Braunschweig, Talk at this conference

12) J. Bell et al., Phys. Rev. D19 (1979) 1

13) R. Brandelik et al., (TASSO), Evidence for charged primary partons in $e^+e^- \to 2$ jets, DESY 81-005

H.C. Ballagh et al., Evidence for hard gluon bremsstrahlung in a deep inelastic neutrino scattering experiment, Contr. paper 194 submitted to this conference.

15) W. Bartel et al., (JADE), Phys. Lett. 101B (1981) 129

16) R. Brandelik (TASSO), Phys. Lett. 105B (1981) 75

17) Ch. Berger (PLUTO), Phys. Lett. 104B (1981) 79

18) W. Bartel (JADE), Phys. Lett. 104B (1981) 325

19) W. Bartel (JADE), Z. Phys. C9 (1981) 315

* I would like to thank Dr. R. Taylor for pointing out to me this reference

C

1) G. Cocconi, Nuovo Cim. 57A (1968) 837

2) F. Cooper et al., Phys. Rev. D11 (1975) 192

3) A.G. Clark et al., Nucl. Phys. B160 (1979) 397

D

1) H. Deden et al., Nucl. Phys. B85 (1975) 269

2) P. Darriulat, Large transverse momentum hadronic processes, Annual Review of Nuclear and Particle Science, 30 (1980) 159

E

1) T. Eichten et al., Phys. Lett. 46B (1973) 274

F

1) E. Fermi, Progr. Theor. Phys. 5 (1950) 570; Phys. Rev. 81 (1951) 683

2) R.P. Feynman, Phys. Rev. Lett. 23 (1969) 1415

3) R. Felst, Talk at this conference

4) H.G. Fischer, Private communication

5) R.D. Field and R.P. Feynman, Nucl. Phys. B136 (1978) 1

6) D. Fournier, Talk at this conference

7) H.G. Fischer, Hadronic high p_T production: can one experimentally disentangle the QCD subprocesses, CERN-EF/80-6

8) G. Flügge, DESY 79/26 (1979)

G

1) R. Göttgens et al., Nucl. Phys. B178 (1981) 392

2) H. Grässler et al., CERN/EP 81-56 (Nucl. Phys. B)

H

1) W. Heisenberg, Z. Phys. 133 (1952) 65

2) R. Hagedorn, Suppl. Nuova Cim. 3 (1965) 147

3) W. Heisenberg, Kosmische Strahlung, Springer-Verlag 1953

4) G. Hanson et al., Phys. Rev. Lett. 35 (1975) 1609

5) R. Hollebeek, Talk at this conference

6) P. Hoyer et al., Nucl. Phys. B161 (1979) 349

L

1) L. Landau, Izv. Akad. Nauk SSSR 17 (1953) 31

M

1) G. Miller et al., Phys. Rev. D5 (1972) 528

2) W.T. Meyer et al., CERN/EP 81-68

3) H. Montgomery, Talk at this conference

4) I. Manelli , "

5) T. Meyer, A Monte Carlo model to produce baryons in e^+e^- annihilation, DESY 81-046

6) P. Mättig (TASSO), Private communication

P

1) D.H. Perkins, Private communication. I would like to thank Prof. Perkins for providing me with this picture.

2) W. Panofsky, Proc. 14th Int. Conf. on High Energy Physics, Vienna 1968

3) K. Pretzl et al., Contr. paper 142 submitted to this conference

4) G. Preparata, Nucl. Phys. B183 (1981) 53

5) PETRA 3-jets
W. Bartel et al., (JADE), Phys. Lett. 91B (1980) 142
D.P. Barber et al, (MARK J), Phys. Rev. Lett. 43 (1979) 830
Ch. Berger et al., (PLUTO), Phys. Lett. 86B (1979) 418
R. Brandelik et al., (TASSO), Phys. Lett. 86B (1979) 243

6) A. Petersen (JADE), Private communication

R

1) P. Renton and W.S.C. Williams, Hadron production in lepton-nucleon scattering, Oxford Preprint OUNP 81-55

S

1) R. Sosnowski, Large p_T phenomena and the strcuture of jets, Proc. 19th Int. Conf. High Energy Physics, Tokyo 1978, p. 693

2) P. Söding, EPS Conference, Geneva 1979, p. 271

3) L. Susskind, Proc. 1977 Int. Symposium on Lepton and Photon Interactions at High Energies, Hamburg, p. 895

4) N. Schmitz, Talk at this conference

5) U.P. Sukhatme, K.E. Lassila and R. Orava, Diquark fragmentation, FERMILAB-PUB-81/20-THY

6) N. Schmitz, Hadron production by neutrinos on protons, MPI-PAE/Exp. El. 88

7) N. Schmitz, Neutrino and antineutrino-nucleon scattering and perturbative quantum chromodynamics, MPI-PAE/Exp-El. 89

8) P. Söding and G. Wolf, Experimental evidence on QCD, DESY 81-013

9) L. Sehgal, Proc. 1977 Int. Symposium on lepton and hadron interactions at high energies, Hamburg, p. 837

10) G. Schierholz and Teper, Baryon production, DESY 81/41

W

1) G. Wolf, Jets in e^+e^- annihilation at high energies, DESY 80/85

Z

1) P. Zerwas, Photon Interactions at short distances, Aachen preprint PITHA 81/12

Further Reading

- R. Orava, Quark jets from deeply inelastic lepton scattering, FERMILAB-Conf.-81/21-EXP
- A. Clegg, An experimental view of jets, Prog. Part. and Nucl. Phys.
- P. Darriulat, Large transverse momentum hadronic processes, Annual Review of Nucl. and Part. Science 30 (1980) 159
- G. Giacomelli and M. Jacob, Phys. Rep. 55 (1979) 1
- G. Wolf, Jets in e^+e^- annihilation at high energies, DESY 80/85
- P. Renton and W.S.C. Williams, Hadron production in lepton nucleon scattering, Oxford Preprint OUNP 81-55

Discussion

B. Esposite, CERN: I would like to make a comment. In your conclusions on low p_T hadron-hadron interactions you pointed out that the leading particle effect has to be subtracted. I certainly agree. But you forgot to say that this has been proposed by the Bologna-CERN-Frascati Collaboration at CERN, which has found and published many results using the method of removing leading protons in pp interactions.

G. Barbiellini, CERN: Can you repeat the argument that explains the high rate of events in the NA5 2π calorimeter trigger?

D. Haidt, DESY: The argument is qualitative and based on the measured topological pp cross sections. If configurations with opposite sided high p_T jets exist, they should be recognizable for jet energies above, say, 6 GeV and contribute to the trigger cross section at $\Sigma E_T \gtrsim 10$ GeV, which is measured in the NA5-experiment to be $\lesssim 10$ μb. At this low cross section level topologies with 30 charged particles are typical (fig. 14). The shape (spherical or clusters or multijets) of these events determines, what fraction gets accepted by the trigger.